Geological Society of America
Memoir 197
2004

# *U-Pb geochronology and geochemistry of a portion of the Mars Hill terrane, North Carolina–Tennessee: Constraints on origin, history, and tectonic assembly*

**Steven E. Ownby***
**Calvin F. Miller***
**Peter J. Berquist**
**Charles W. Carrigan***
*Department of Geology, Vanderbilt University, Nashville, Tennessee 37235, USA*
**Joseph L. Wooden**
*USGS-SUMAC Ion Probe Lab, Green Building, Stanford University, Stanford, California 94305-2220, USA*
**Paul D. Fullagar**
*Department of Geological Sciences CB# 3315, University of North Carolina, Chapel Hill, North Carolina 27599-3315, USA*

## ABSTRACT

**The Mars Hill terrane (MHT), a lithologically diverse belt exposed between Roan Mountain, North Carolina–Tennessee, and Asheville, North Carolina, is distinct in age, metamorphic history, and protoliths from the structurally overlying Eastern Blue Ridge and underlying Western Blue Ridge. MHT lithologies include diverse granitic gneisses, abundant mafic and sparse ultramafic bodies, and mildly to strongly aluminous paragneisses. These lithologies experienced metamorphism in the granulite facies and are intimately interspersed on cm to km scale, reflecting both intrusive and tectonic juxtaposition.**

**Previous analyses of zircons by high-resolution ion microprobe verified the presence of Paleoproterozoic orthogneiss (1.8 Ga). New data document a major magmatic event at 1.20 Ga. Inherited and detrital zircons ranging in age from1.3 to 1.9 Ga (plus a single 2.7-Ga core), ubiquitous Sm-Nd depleted mantle model ages ca. 2.0 Ga, and strongly negative $\varepsilon_{Nd}$ during Mesoproterozoic time all attest to the pre-Grenville heritage of this crust that was suggested by previous whole-rock Pb and Rb-Sr isotope studies. A single garnet amphibolite yielded a magmatic age of 0.73 Ga, equivalent to the Bakersville dike swarm, which cuts both the MHT and the adjacent Western Blue Ridge. Zircons from this sample display 0.47-Ga metamorphic rims. Zircons from all other samples have well-developed ca. 1.0-Ga metamorphic rims that date granulite-facies metamorphism. Silica contents of analyzed samples range from 45 to 76 wt %, reflecting the extreme diversity observed in the field and the highly variable protoliths.**

**The MHT contrasts strikingly with basement of the adjacent Eastern and Western Blue Ridge, which comprise relatively homogeneous, 1.1- to 1.2-Ga granitic rocks**

*Corresponding author: Miller, calvin.miller@vanderbilt.edu; present address, Carrigan and Ownby: Department of Geological Sciences, University of Michigan, Ann Arbor, Michigan 48109.

Ownby, S.E., Miller, C.F., Berquist, P.J., Carrigan, C.W., Wooden, J.L., and Fullagar, P.D., 2004, U-Pb geochronology and geochemistry of a portion of the Mars Hill terrane, North Carolina–Tennessee: Constraints on origin, history, and tectonic assembly, *in* Tollo, R.P., Corriveau, L., McLelland, J., and Bartholomew, M.J., eds., Proterozoic tectonic evolution of the Grenville orogen in North America: Boulder, Colorado, Geological Society of America Memoir 197, p. 609–632. For permission to copy, contact editing@geosociety.org. 

**with initial $\varepsilon_{Nd}$ values near 0. It appears to have more in common with distant Paleoproterozoic crustal terranes in the Great Lakes region, the southwestern United States, and South America.**

**Keywords:** Appalachians, geochemistry, zircon, SHRIMP, geochronology, Proterozoic, granulite facies, Grenville, Nd isotopes

## INTRODUCTION

The Blue Ridge province of the southern Appalachian orogen is divided into western (Western Blue Ridge) and eastern (Eastern Blue Ridge) zones. The Western Blue Ridge is generally thought to be part of Laurentia (native North America), whereas the more structurally and lithologically complex Eastern Blue Ridge is considered to comprise one or more suspect terranes—possibly a rifted and reattached fragment of Laurentia or an exotic terrane(s) (e.g., Hatcher, 1989; Stewart et al., 1997). The Western Blue Ridge includes granitic rocks of Grenville and Neoproterozoic age; Neoproterozoic mafic dikes and intrusions; and overlying, chemically mature metasedimentary rocks that experienced relatively low-grade Paleozoic metamorphism (e.g., Rankin, 1975; Hatcher, 1978; Misra and McSween, 1984; Davis, 1993). The Eastern Blue Ridge comprises an assemblage of less mature, Neoproterozoic–early Paleozoic clastic metasedimentary rocks and mafic to ultramafic bodies of higher metamorphic grade; variably deformed, felsic Paleozoic intrusions; and relatively sparse exposures of Grenville-age granitoid gneisses.

Several workers have noted an assemblage of lithologies at the Eastern Blue Ridge–Western Blue Ridge boundary that, although included by some as part of the Western Blue Ridge, appears to have no counterpart in either area. This assemblage is exposed in a belt that extends at least from the vicinity of Roan Mountain, Tennessee–North Carolina, to northwest of Asheville, North Carolina (Fig. 1) (Merschat, 1977; Gulley, 1982; Bartholomew and Lewis, 1988, 1992; Raymond et al., 1989; Merschat and Wiener, 1990; Johnson, 1994; Raymond and Johnson, 1994; Adams et al., 1995; Stewart et al., 1997; Trupe et al., 2001). It differs from the Eastern Blue Ridge and Western Blue Ridge as follows:

1. The MHT displays widespread evidence for granulite-facies metamorphism (e.g., Merschat, 1977; Gulley, 1985; Adams and Trupe, 1997); granulite-grade rocks are rare in the Eastern and Western Blue Ridge.

2. The MHT contains abundant mafic and some ultramafic rocks interspersed with granitic gneisses on the cm to km scale; the mafic rocks are commonly migmatitic (e.g., Merschat, 1977). Mafic rocks are common in the Eastern Blue Ridge, but only in contact with the metasedimentary sequences, and they are rarely migmatitic; they are rare or absent in the Western Blue Ridge, except for the Neoproterozoic dikes.

3. Field relations and Rb-Sr geochronology suggest that the MHT contains the oldest rocks in the southern Appalachians and lacks Phanerozoic rocks. Metasedimentary rocks that have experienced granulite-facies metamorphism are cut by lower-grade, 730-Ma dikes of the Bakersville swarm (Goldberg et al., 1986), and a whole-rock Rb-Sr isochron has been interpreted to demonstrate a magmatic crystallization age of 1.8 Ga at one locality (Monrad and Gulley, 1983). Whole-rock lead isotope ratios (Sinha et al., 1996) and high initial strontium isotope ratios (Monrad and Gulley, 1983; Fullagar et al., 1979) also suggest antiquity of this terrane. All metasedimentary rocks in the Eastern Blue Ridge and Western Blue Ridge are interpreted to be younger than 730 Ma, and no other igneous rocks from the southeastern United States has reported radiometric ages older than 1.2 Ga.

4. The Mars Hill terrane (MHT) is the most lithologically diverse basement exposure south of Virginia. Other basement exposures in this region are almost entirely meta-igneous (possibly including some high-grade, feldspathic metasandstone) and generally lack mafic rocks.

Based upon its lithologic distinctiveness, the MHT has been mapped as an important regional unit (or units) and interpreted as a suspect terrane. Merschat (1977) mapped biotite-hornblende migmatite in the vicinity of Mars Hill, North Carolina, and inferred that it was regionally extensive. Gulley (1982, 1985) investigated granulite-facies rocks at Roan Mountain and informally designated metasedimentary lithologies as Cloudland gneiss and mafic and felsic meta-igneous rocks as Carvers Gap gneiss. On the North Carolina state geologic map (Brown

Figure 1. (A) Location of the MHT and its possible extent toward Georgia and Virginia. (B) Localities of samples analyzed for this study and Carrigan et al. (2003). Sample labels all have prefix RM, except for MBCL4 and 5. Inset: Roan Mountain-Bakersville area, where most samples were collected. North Carolina State Highway 261, Tennessee State Highway 143, and Roan Mountain spur road (Forest Service Route 130) are shown for reference. CG—Carvers Gap; MM—Meadlock Mountain; RHB—Roan High Bluff. Only samples for which analytical data are reported are shown. For all samples shown, elemental analyses were done; for circled samples, Rb-Sr-Sm-Nd isotopic analyses; for underlined samples, zircon U-Pb analyses; samples with asterisks were analyzed by Carrigan et al. (2003). Zircon sample CAR 1501 was collected by J.P. Dubé and K.G. Stewart at locality RM2X. Maps modified from Brown et al. (1985) and K.G. Stewart (unpublished data).

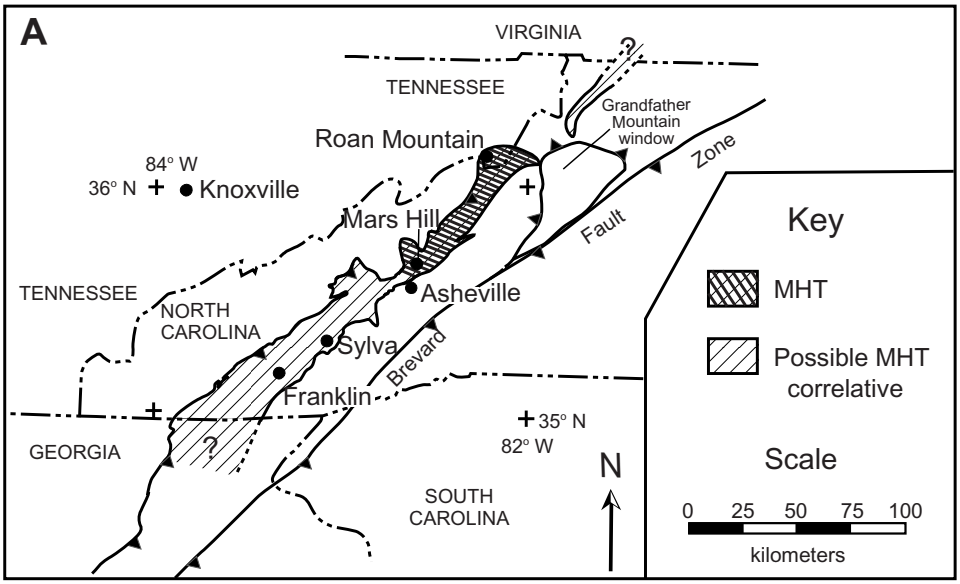
A
VIRGINIA
TENNESSEE
Grandfather Mountain window
Roan Mountain
84° W
36° N
Knoxville
Mars Hill
Zone
Fault
Asheville
TENNESSEE
NORTH CAROLINA
Sylva
Brevard
Franklin
35° N
82° W
GEORGIA
SOUTH CAROLINA
N
Key
MHT
Possible MHT correlative
Scale
0 25 50 75 100
kilometers

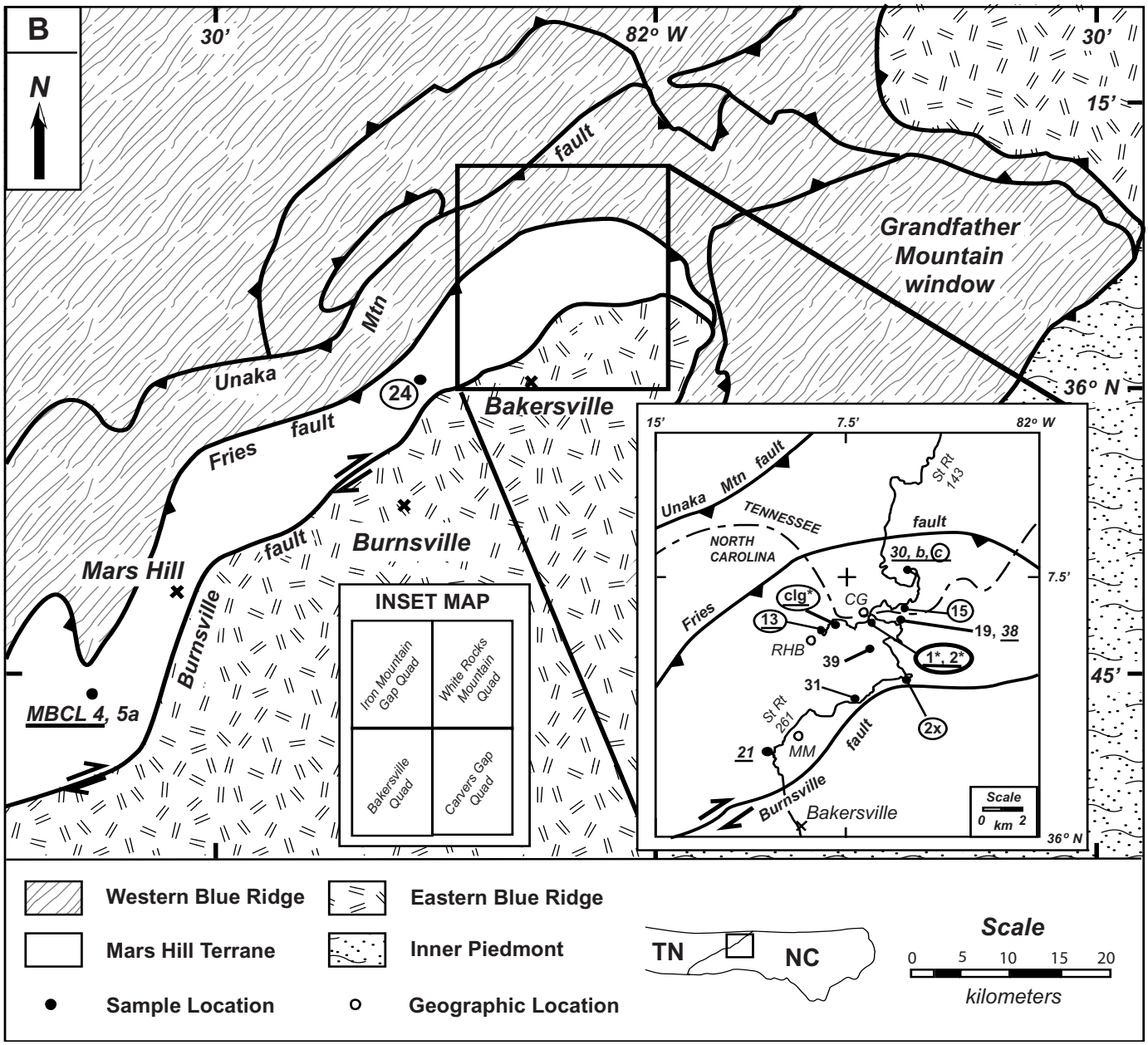
B
N
30'
82° W
30'
15'
fault
Grandfather Mountain window
Mtn
Unaka
24
Bakersville
36° N
Fries
fault
Burnsville
fault
Mars Hill
Burnsville
MBCL 4, 5a
45'
INSET MAP
Iron Mountain Gap Quad
White Rocks Mountain Quad
Bakersville Quad
Carvers Gap Quad
15'
7.5'
82° W
Unaka
Mtn
fault
TENNESSEE
NORTH CAROLINA
St Rt 143
fault
30, b, c
7.5'
Fries
clg*
CG
13
15
19, 38
RHB
39
1*, 2*
31
2x
St Rt 261
21
MM
fault
Burnsville
Bakersville
Scale
0 km 2
36° N
Western Blue Ridge
Eastern Blue Ridge
Mars Hill Terrane
Inner Piedmont
Sample Location
Geographic Location
TN
NC
Scale
0 5 10 15 20
kilometers

et al., 1985), Merschat's biotite-hornblende migmatite unit stretches for 80 km, from Roan Mountain to northwest of Asheville, and similar, possibly related migmatitic biotite gneiss extends another 120 km southwest to the Georgia border (Raymond et al., 1989). Workers from the University of North Carolina at Chapel Hill have mapped the northern portion of this zone as the Pumpkin Patch or Fries thrust sheet and refer to the high-grade rocks as the Pumpkin Patch Metamorphic Suite (Goldberg et al., 1989; Adams et al., 1995; Stewart et al., 1997; Trupe et al., 2001). Bartholomew and Lewis (1988, 1992), Raymond (1987; Raymond et al., 1989), and Brewer and Woodward (1988) identified this general area as a suspect terrane, calling it the Mars Hill terrane, the Cullowhee terrane, and Amphibolitic Basement Complex, respectively. Raymond et al. (1989) and Brewer and Woodward (1988) suggested that the terrane may be a melangelike complex of granitic and mafic material, minutely imbricated as a consequence of ocean basin closure. Raymond et al. (1989) suggested that closure occurred during the late Neoproterozoic–early Paleozoic (post-Bakersville dikes), whereas Brewer and Woodward (1988) interpreted it to have been completed during late Mesoproterozoic–early Neoproterozoic time (pre-Bakersville dikes).

In a reconnaissance study of basement rocks of western North Carolina and northernmost Georgia and South Carolina, Carrigan (2000) and Carrigan et al. (2000, 2001, 2003) noted that Western Blue Ridge and Eastern Blue Ridge basement is uniformly broadly granitic in composition. Zircons from these rocks lack inheritance, yield magmatic ages between 1.08 and 1.19 Ga, and have ca. 1.03-Ga metamorphic rims. An initial $\varepsilon_{Nd}$ value near 0 suggests that the crust that these rocks represent was young and possibly juvenile during Grenville time. Only in the MHT did Carrigan identify an older component, with both U-Pb and Sm-Nd data suggesting the presence of Paleoproterozoic crust; this is consistent with the initial Rb-Sr results of Monrad and Gulley (1983) and whole-rock Pb isotope data of Sinha et al. (1996).

The purpose of this paper is to characterize the geochemistry and ages of representative examples of lithologies from the MHT in its better-documented portion between Roan Mountain and Asheville, in order to decipher its geologic history and constrain its relationships with surrounding units. These data will, in turn, contribute to a better understanding of the Proterozoic and Paleozoic assembly of southeastern North America.

## METHODS

Samples for both geochronological (5 kg) and geochemical (1 kg) analysis were selected from fresh outcrops to represent both typical lithologies and the diversity of compositions. Sample CAR 1501 had been collected previously by J.P. Dubé and K.G. Stewart. Sample locations are shown in Figure 1, B; precise locations and petrographic descriptions can be found in Ownby (2002).

Zircons were separated using standard procedures, mounted in epoxy, polished, and imaged by cathodoluminescence on the JEOL JSM 5600 scanning electron microscope at Stanford University. Points on the zircon grains ~30–40 μm in diameter were analyzed according to Stanford/U.S. Geological Survey (USGS) Sensitive High-Resolution Ion Microprobe, Reverse Geometry (SHRIMP-RG) Facility procedures (cf. Bacon et al., 2000). Zircon standards R33 (419 Ma) and CZ3 (550 ppm U) were used for U-Pb and U concentration standards, respectively. Standards were provided by the Stanford/USGS facility. Common Pb corrections were based on measured $^{204}$Pb and data reduction used SQUID (Version 1.02; Ludwig, 2001).

Powders prepared in an alumina ceramic shatterbox were analyzed for elemental and isotopic analyses. Elemental compositions were determined by Activation Laboratories, Ltd., of Canada, using X-ray fluorescence, inductively coupled plasma mass spectrometry, and instrumental neutron activation analysis. Sm-Nd and Rb-Sr isotopic analyses were performed at the University of North Carolina at Chapel Hill on a VG Micromass Sector 54 multicollector thermal ionization mass spectrometer, following the methods described in Fullagar et al. (1997) and Fullagar and Butler (1979).

## PROTOLITH INTERPRETATION: PITFALLS, CRITERIA USED, AND KEY ISSUES

Interpretation of protoliths in the MHT faces formidable obstacles. Primary textures have been obliterated by high-temperature recrystallization, and for the most part, intense ductile deformation has thoroughly modified initial rock-unit geometry and destroyed primary contact relations and textures (see the Petrography and Field Relations section). In this paper, we rely primarily on elemental chemistry for protolith interpretation. Mafic rocks are relatively straightforward: their geochemistry is indistinguishable from common basalts and gabbros and is unlike any common sediments. Likewise, sparse, highly aluminous rocks are clearly metapelites (we have analyzed only a single sample, although Gulley [1982] described numerous samples from the Cloudland gneiss). Other unequivocal protoliths are absent: there are no high-silica rocks (>80 wt % $SiO_2$), carbonates, or calc-silicates among our samples.

A majority of the rocks of the MHT are feldspar-rich gneisses and granofelses that are intermediate to felsic (55–75 wt % $SiO_2$) and mildly metaluminous to moderately peraluminous (Fig. 2). Potential protoliths of such rocks include intermediate to felsic igneous rocks and feldspathic sandstones (greywackes, arkoses). There is no entirely reliable way to distinguish igneous rocks from sandstones, because extremely immature sandstones can be identical to their igneous sources. However, there is a strong tendency for clastic sediments to show the imprint of weathering and sorting and therefore to be enriched in quartz and more peraluminous than igneous source rocks. Recognizing that these criteria are not foolproof, we dis-

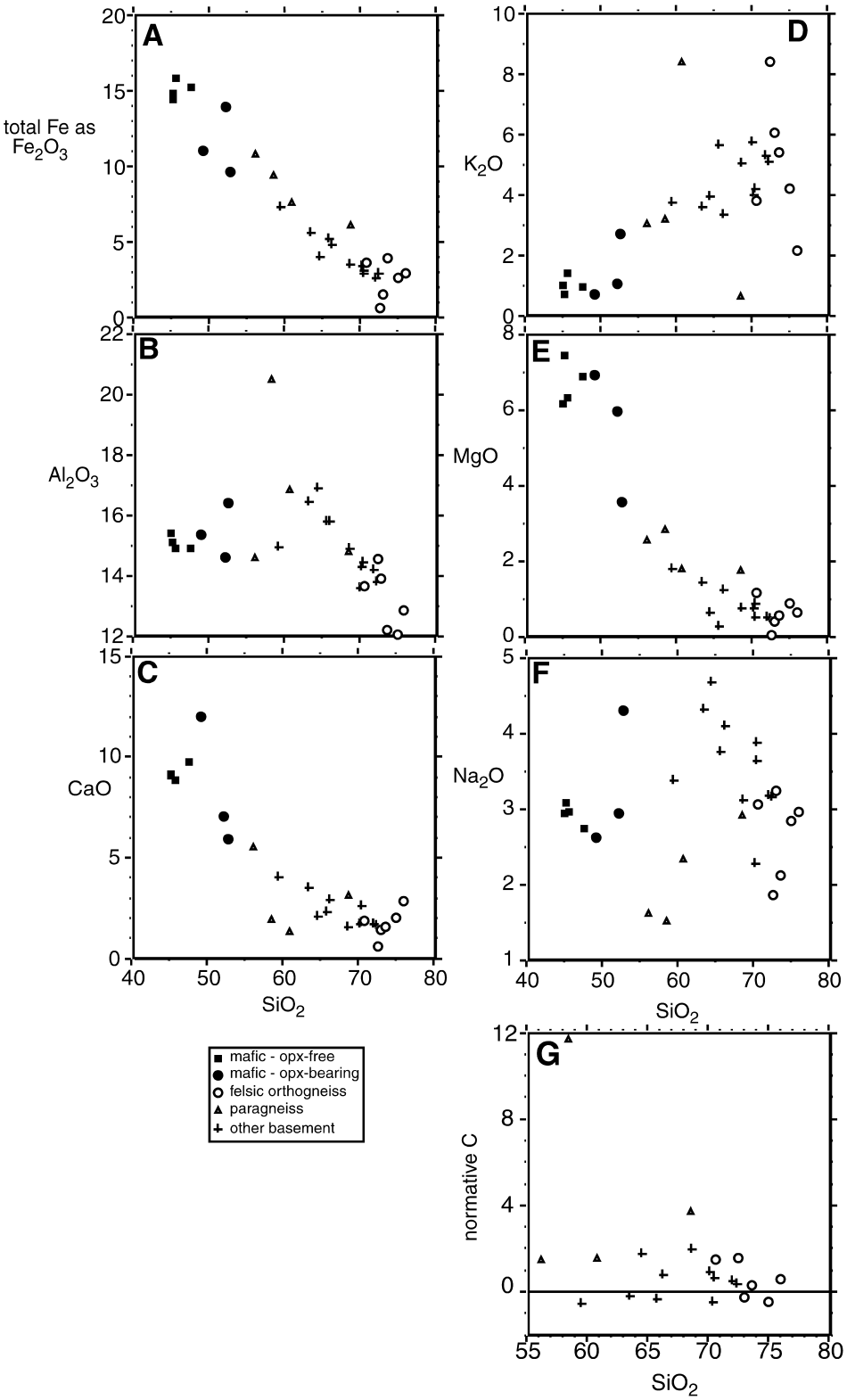


Figure 2. Selected major-element oxides and normative corundum plotted against $SiO_2$. All concentrations in wt %. Negative normative corundum in panel G is the deficiency in alumina realtive to CaO + $Na_2O$ + $K_2O$ in metaluminous samples (calculated from the same equation as normative corundum). "Other basement" includes Eastern Blue Ridge and Western Blue Ridge basement, from Carrigan (2000) and Carrigan et al. (2003).

tinguish probable sedimentary from igneous protoliths on the following basis: rocks with typical intermediate to felsic igneous $SiO_2$ and $Al_2O_3$ concentrations (55–75 and 10–20 wt %, respectively) are considered likely to have igneous protoliths if they do not have unusually high normative corundum (>0 at 55 wt % $SiO_2$, >2 wt % at 75 wt % $SiO_2$) or normative quartz (>10 at 55 wt % $SiO_2$, >45 wt % at 75 wt % $SiO_2$). Rocks that meet these standards have >50% normative feldspar, also consistent with igneous parentage. A further geochemical test of protoliths, presented in Figure 3, results in the same protolith assignments as the abovementioned criteria for all but one sample. Previous studies in the area have taken similar approaches and concluded that, with the exception of the Cloudland gneiss, igneous protoliths dominate the MHT (Merschat, 1977; Gulley, 1982), although in a review paper, Bartholomew and Lewis (1988) suggested that it is largely metasedimentary.

We emphasize that distinguishing volcanic from plutonic protoliths on the basis of geochemistry is impossible. In some exposures in the MHT, intrusive relationships permit the identification of plutonic rocks, but in most cases the distinction cannot be made.

Zircon age distributions and zoning patterns can also suggest protolith. Excluding metamorphic rims, a single dominant age population is consistent with igneous parentage, although sediment derived from a single-aged source terrane could yield the same result. A modest number of distinctly older zones, especially if they are clearly located within a core, are also consistent with an igneous protolith. Absence of a dominant age population or older ages that are more common than younger ones strongly suggests sedimentary origin. Likewise, fragmented grains may suggest sedimentary transport. Rounded external zircon morphology, however, is an unreliable criterion for sedimentary origin in rocks with histories like these: inherited cores in igneous rocks typically are rounded by resorption; zircons from very high-grade rocks characteristically have thick overgrowths that impart a subrounded external shape, and partial resorption rounds premetamorphic cores (e.g., Hanchar and Miller, 1993). Zircon data presented in this paper and observed morphologies are mostly consistent with geochemically based protolith assignment; exceptions are discussed in the Geochronology section.

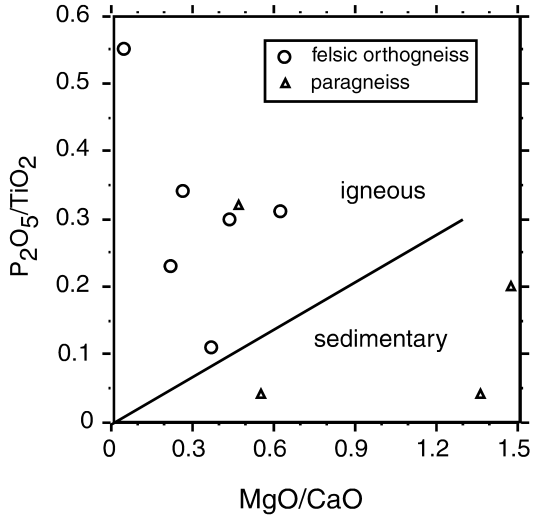


Figure 3. $P_2O_5/TiO_2$ plotted against MgO/CaO as a discriminator for felsic igneous versus clastic sedimentary protoliths in granulite-facies rocks. After Werner (1987).

Protolith interpretation is of special interest in two cases: sample RM1, collected along the National Forest spur road 130 to the top of Roan Mountain, and the RM30 exposure (three dated samples) along Tennessee Highway 143, northeast of Roan Mountain. The RM30 exposure and samples are discussed in following sections on field relations, geochemistry, and geochronology. RM1 is a key sample reported in Carrigan et al. (2003) and interpreted as a meta-igneous rock with an age of 1.8 Ga. Only at Roan Mountain has there been a suggestion of rocks of this antiquity in the southeastern United States, and the Carrigan et al. data appear to confirm previous suggestions. If it is in fact metasedimentary, then this age points to an Early Proterozoic source region, but does not verify the existence here of Early Proterozoic rocks. The sample is of massive, unfoliated granofels. The rationale for its interpretation as meta-igneous is as follows:

1. The Carvers Gap gneiss, of which RM1 is part, was interpreted as an igneous complex by Gulley (1982), based primarily on geochemical criteria similar to those discussed above.
2. Previous efforts at dating suggested essentially the same age: Monrad and Gulley (1983) presented a whole-rock Rb-Sr isochron based on samples collected along a 1.5-km road cut traverse that included samples from near site RM1; the isochron appears to be robust and yielded an age of 1.82 Ga, an unlikely result if these were metasedimentary rocks. Furthermore, Fullagar and Gulley (1999) reported a conventional zircon U-Pb upper intercept of 1.84 Ga and lower intercept of 1.08 Ga for a nearby sample.
3. Eight of nine of zircon core analyses of Carrigan et al. (2003) define a discordia with an upper intercept of 1.77 Ga and lower intercept of 1.01 Ga; the only analysis that did not fall on this discordia gave a discordant post-Grenville age and clearly reflected younger lead loss. The well-defined discordia would require that, if this rock were metasedimentary, it had only a single detrital age population and that this population be distinct from detrital populations of all other reported samples form the Southeast (e.g., see Carrigan et al., 2003; Bream et al., this volume, and data in this paper).
4. Internal zoning in zircons from sample RM1 is clearly igneous and, although all grains have metamorphic overgrowths, the magmatic interiors are not truncated, as would be likely in detrital populations (see Fig. 4 *in* Carrigan et al., 2003).
5. The composition of RM1, although fairly high in $SiO_2$ (75.8 wt %), is within a reasonable igneous range; it is very weakly peraluminous, with only 0.6 wt % normative corundum, and has >50% normative feldspar. We acknowledge that RM1

*could* be a highly immature meta-arkose, but the preponderance of evidence strongly suggests that it is a meta-igneous rock and supports the notion that there is a 1.8-Ga igneous complex at Roan Mountain.

## PETROGRAPHY AND FIELD RELATIONS

The MHT is characterized by a great diversity of lithologies interspersed on all scales. Almost every exposure contains multiple rock types, some with readily interpretable contact relations (dikes, migmatitic leucosomes and melanosomes, pervasive injection zones), but many others with more ambiguous relationships that, at least in some cases, require tectonic juxtaposition. Raymond et al. (1989) described and illustrated exposures in possible correlative rocks to the southwest of Asheville that show similar juxtapositions of lithologies, which they refer to as "block-in-matrix" structures.

Mafic rocks are ubiquitous throughout the MHT. The most readily interpretable are dikes of the Neoproterozoic Bakersville dike swarm (Goldberg et al., 1986; Adams and Trupe, 1997), which crosscut other lithologies and are apparently the youngest rocks of the MHT. Although they commonly preserve relict fine-grained diabasic fabric, the dike rocks are overprinted by amphibolite-facies, garnet amphibolite, and mineral assemblages. Larger mafic bodies that preserve igneous textures have been interpreted as Bakersville suite intrusions (Goldberg et al., 1986; Adams and Trupe, 1997). The Meadlock Mountain gneiss, a biotite-bearing garnet ± clinopyroxene amphibolite, is unusual in that it forms mappable-scale bodies. Adams et al. (1995) reported that it records peak conditions in the high-*P* portion of the amphibolite facies (13 kb, 725 °C), consistent with the presence of felsic leucosome pods that suggest anatexis during peak metamorphism. Garnet amphibolites lacking orthopyroxene are fairly widespread in the MHT and may correlate with Meadlock Mountain gneiss. Orthopyroxene (opx)-bearing mafic rocks are also abundant, but appear not to form extensive exposures. Gulley (1985) estimated peak granulite-facies conditions for the opx-bearing metabasites and nearby metapelites at Roan Mountain as ~7 kb, 800 °C. The granulite-grade mafic rocks are commonly banded, either with alternating hornblende-rich and opx-rich layers, or with more- and less-felsic layers. In thin section, a garnet-hornblende assemblage rims or replaces opx, indicating a retrograde reaction (lower *T* and/or higher *P*). Ultramafic rocks are present locally (Merschat, 1977; Raymond and Johnson, 1994), but they are exceedingly rare in areas that we sampled (we collected only a single igneous-textured, plagioclase-bearing websterite). We interpret the Bakersville dikes, and probably the larger mafic bodies (Meadlock Mountain gneiss), to be intrusions. It is not evident whether smaller sheets and pods are metamorphosed volcanic rocks, sills, or dismembered dikes and larger intrusions.

Like mafic rocks, felsic gneisses are ubiquitous but variable in field characteristics and composition. None appear to form map-scale plutons. Some are compositionally banded; in others, foliation is defined by weak mafic mineral alignment or by mylonitic fabric; and still others are massive, with prominent, blocky, perthitic K-feldspar. Compositional banding probably reflects both transposed compositional layering in protoliths and deformation-induced metamorphic segregation; protoliths appear to include aluminous sediments, very small intrusions, and probably felspathic psammites, felsic volcanic rocks, and dismembered larger intrusions. Some are rich in K-feldspar (alkali feldspar granite composition), others are very poor in Kspar (trondhjemitic); most are quartz-rich, but not rich enough to represent quartz-rich sandstone; and some are rich in kyanite and/or sillimanite (Gulley, 1985). Biotite is present in all samples. Opx and clinopyroxene, present in some but not all samples, document the granulite-facies event in the MHT. Where present, the pyroxenes are commonly rimmed by garnet and hornblende, probably reflecting the high-*P* amphibolite-facies event described by Adams et al. (1995) for mafic rocks. Garnet is also commonly present as discrete grains.

Some of the feldspathic banded gneisses are similar to MHT gneisses exposed near Mars Hill that are interpreted as metavolcanics (Merschat and Carter, personal communication) but, in these intensely deformed and metamorphosed rocks, distinguishing volcanic from intrusive or weakly aluminous sandstone protoliths is difficult (see the Protolith Interpretation and Geochemistry sections for discussion of the distinction between sedimentary and igneous protoliths). Small bodies of massive felsic rock intrude mafic and banded gneisses, indicating that the protoliths were granites. A single plagioclase-biotite-quartz-garnet-scapolite-ilmenite(?) banded gneiss sample (RM13) is of enigmatic origin. Highly aluminous paragneisses with probable shale and aluminous graywacke protoliths are common on Roan Mountain (Gulley, 1985) but rare elsewhere.

The latest events indicated by field and petrographic relations to have affected the MHT include development of local mylonitic shear zones that preserve some unrecovered strain and limited greenschist-facies recrystallization, indicated by minor epidote and fine-grained chlorite, muscovite, and biotite (Gulley, 1985; Adams and Trupe, 1997).

One exposure along Tennessee Highway 143 merits a brief discussion, because it is the site at which three samples (RM30, RM30B, RM30C) were collected that yielded important but somewhat equivocal geochemical and geochronological data. This road-cut exposure lacks the rather chaotic block-in-matrix structure that characterizes much of the MHT, but contact relations among lithologic units are still not straightforward. The road cut is dominated by banded gneiss, mostly gray and intermediate to felsic in appearance (represented by RM30B) and, in part, distinctly more mafic (RM30C). The gray gneiss is mineralogically simple, with feldspars, biotite, quartz, and garnet. The mafic gneiss contains plagioclase, hornblende, clinopyroxene, opx, garnet, biotite, and quartz. Sheets of massive, medium-coarse, felsic granofels up to ~2 m in thickness parallel the foliation of the gneisses. RM30, collected from one of these sheets, comprises abundant feldspars and quartz, with minor biotite,

opx, and clinopyroxene. The gneisses and granofels are cut by a fine-grained mafic dike that is probably part of the Bakersville swarm. It is not obvious whether the planar contacts and sheet-like geometry of the three predike lithologies reflect original forms and contacts of the units or tectonic rearrangement and transposition. If the initial geometry is more or less intact, the most reasonable field interpretations are that either (1) all three are part of a depositional sequence—volcanic or sedimentary; or (2) the banded gneisses were intruded by dikes or sills of the granitic granofels protolith (or, conceivably, that the gray banded gneiss was intruded by both the granofels protolith and the mafic gneiss protolith).

## GEOCHEMISTRY

Elemental compositions of MHT rocks reflect the lithologic diversity that is evident in the field and constrain possible protoliths (Table 1; Figs. 2–5). Concentrations of $SiO_2$ in the analyzed samples range from 45 to 76 wt %. The samples with <55 wt % $SiO_2$ have compositions consistent with mafic magmatic heritage; they have moderately high $Al_2O_3$, Cr, Ni, and Mg#s (atomic Mg/[Mg + Fe], 0.4–0.6) and are metaluminous and olivine-normative to weakly quartz-normative (Ownby, 2002). In Table 1, Figures 2 and 4–6, and the discussion that follows, these rocks are interpreted to be metamorphosed mafic igneous rocks—diabases, basalts, and/or gabbros—and are subdivided into opx-bearing and opx-free varieties. Compositions of rocks with 70 to 76 wt % $SiO_2$ suggest felsic igneous protoliths: they have abundant normative feldspar and 27 to 43 wt % normative quartz and are weakly metaluminous to weakly peraluminous. As noted previously, we cannot rule out the possibility that some of these samples are metamorphosed, extremely immature arkoses or volcaniclastic sediments that closely mimic their igneous sources in composition, but the simplest and most plausible interpretation is that most or all are metagranitoids and metarhyolites. Therefore, we refer to them as felsic orthogneisses.

The four analyzed samples with 56 to 69 wt % $SiO_2$ are all dissimilar to typical igneous rocks. Compared with igneous rocks with similar $SiO_2$ concentrations, all four are unusually peraluminous, three are unusually high in normative quartz, and three have high Cr and Ni (Table 1; Fig. 2, G) (Ownby, 2002). The peraluminous compositions are a reflection of very low $Na_2O$ and/or CaO concentrations. On a plot of $P_2O_5/TiO_2$ versus MgO/CaO, three samples plot clearly in the metasedimentary field, whereas all samples interpreted to be felsic orthogneisses plot in the igneous field (Fig. 3) (Werner, 1987). Sample RM31, with extremely high normative corundum and moderate $SiO_2$, clearly has a pelitic protolith, similar to fairly common lithologies at Roan Mountain described by Gulley (1982, 1985). RM-CLG, a sample of Gulley's Cloudland paragneiss, is also almost certainly metasedimentary, based on its high normative corundum and quartz and concentrations of Ni and Cr; its probable protolith is an impure sandstone, perhaps a quartz-rich greywacke. RM30B has 1.5 wt % normative corundum, very low $Na_2O$ and Sr concentrations, and high Cr and Ni, characteristics that are highly unusual for an igneous rock with 61 wt % $SiO_2$. We therefore suggest that it is also a metagreywacke (RM30B is discussed further in the following paragraph). RM13 has a highly unusual composition that does not match either typical igneous or sedimentary protoliths; despite having 56 wt % $SiO_2$, it has low Mg# (0.3), Cr, and Ni, extremely low $Na_2O$, and is peraluminous. It also is enriched in Sr, Ba, $P_2O_5$, and $TiO_2$. This sample may have been derived from an unusual sediment that included both chemically precipitated and insoluble residue components, or it could represent an intensely altered protolith. Because its composition appears to reflect surface or near-surface processes, we group it tentatively with the paragneisses.

Elemental chemistry of the samples from the RM30 road cut on TN Highway 143 suggests that this exposure contains both igneous and sedimentary rocks. RM30B, the gray banded gneiss, is probably metasedimentary, as noted earlier. Mafic banded gneiss RM30C has an igneous composition; it could be a sill or transposed dike, but the simplest interpretation is that it was a basalt flow interbedded with immature sandstones. RM30 has a felsic igneous composition and therefore, its protolith could have been a rhyolitic ash or lava or a dike or sill. Its high Zr concentration (711 ppm) could suggest that it is a metasand-

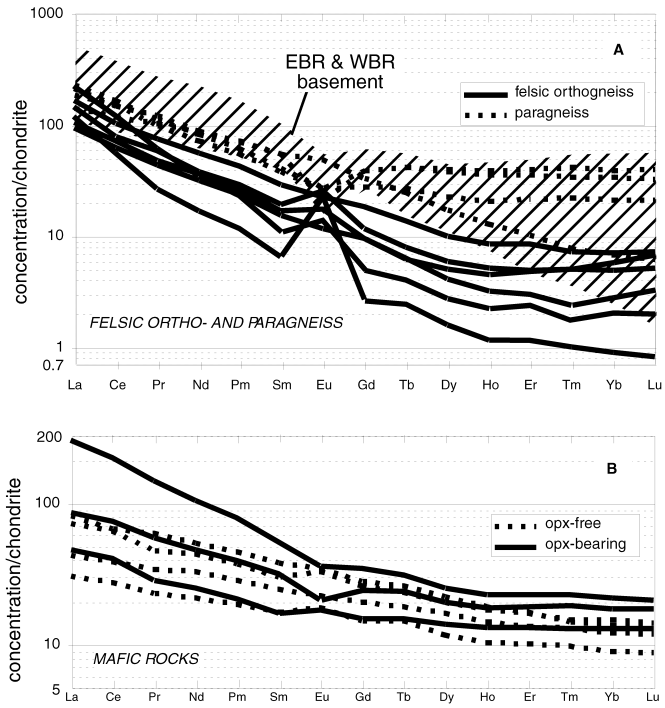


Figure 4. Chondrite-normalized REE abundances (normalization following Boynton, 1984). The field of Eastern Blue Ridge (EBR) and Western Blue Ridge (WBR) basement is from Carrigan (2000) and Carrigan et al. (2003).

## TABLE 1. ELEMENTAL DATA

| | Sample number | | | | | | | | | | | | | | | | |
|---|---|---|---|---|---|---|---|---|---|---|---|---|---|---|---|---|---|
| | Mafic opx-free | | Mafic opx-bearing | | | | Felsic orthogneiss | | Paragneiss | | | | | | | | |
| | RM2* | RM2X | RM19 | RM39 | RM24 | RM30C | MBCL5A | RM1* | RM15 | RM21 | RM30 | RM38 | MBCL4 | RM13 | RM30B | RM31 | RM–CLG* |
| $SiO_2$, wt% | 47.40 | 45.44 | 44.87 | 45.01 | 48.97 | 52.02 | 52.52 | 75.79 | 72.32 | 74.83 | 73.40 | 70.45 | 72.76 | 56.01 | 60.65 | 58.35 | 68.48 |
| $Al_2O_3$ | 14.89 | 14.90 | 15.38 | 15.10 | 15.32 | 14.59 | 16.38 | 14.54 | 12.03 | 12.17 | 13.62 | 13.90 | 14.59 | 16.81 | 20.50 | 14.76 | |
| $Fe_2O_3$ (total) | 15.12 | 15.72 | 14.35 | 14.77 | 10.94 | 13.84 | 9.52 | 2.81 | 0.54 | 2.56 | 3.81 | 3.54 | 1.47 | 10.71 | 7.54 | 9.39 | 6.05 |
| MnO | 0.20 | 0.22 | 0.22 | 0.21 | 0.18 | 0.20 | 0.15 | 0.06 | 0.00 | 0.04 | 0.02 | 0.04 | 0.02 | 0.11 | 0.08 | 0.17 | 0.11 |
| MgO | 6.85 | 6.32 | 6.15 | 7.42 | 6.91 | 5.96 | 3.56 | 0.61 | 0.02 | 0.87 | 0.55 | 1.14 | 0.37 | 2.56 | 1.80 | 2.81 | 1.73 |
| CaO | 9.69 | 8.84 | 9.05 | 9.14 | 11.96 | 7.02 | 5.91 | 2.85 | 0.54 | 2.02 | 1.53 | 1.84 | 1.40 | 5.48 | 1.32 | 1.91 | 3.13 |
| $Na_2O$ | 2.73 | 2.95 | 2.94 | 3.07 | 2.61 | 2.94 | 4.30 | 2.96 | 1.85 | 2.83 | 2.11 | 3.06 | 3.23 | 1.61 | 2.33 | 1.51 | 2.91 |
| $K_2O$ | 0.91 | 1.36 | 0.97 | 0.70 | 0.66 | 1.04 | 2.69 | 2.15 | 8.37 | 4.16 | 5.37 | 3.80 | 6.05 | 3.04 | 8.40 | 3.16 | 0.61 |
| $TiO_2$ | 2.49 | 2.94 | 3.10 | 2.34 | 1.00 | 1.36 | 2.33 | 0.27 | 0.07 | 0.43 | 0.64 | 0.51 | 0.26 | 3.63 | 0.93 | 1.13 | 0.80 |
| $P_2O_5$ | 0.25 | 0.41 | 0.50 | 0.19 | 0.10 | 0.16 | 0.85 | 0.06 | 0.04 | 0.13 | 0.07 | 0.16 | 0.09 | 1.16 | 0.04 | 0.23 | 0.03 |
| LOI | –0.09 | –0.13 | 1.45 | 0.58 | 0.30 | 0.30 | 0.89 | 0.12 | 0.94 | 0.26 | 0.30 | 1.59 | 0.36 | 0.58 | 0.12 | 1.09 | 0.10 |
| Total | 100.44 | 98.96 | 98.99 | 98.52 | 98.95 | 99.42 | 99.10 | 100.49 | 99.21 | 100.14 | 99.97 | 99.73 | 99.91 | 99.49 | 100.03 | 100.25 | 98.72 |
| normal C† | –7.64 | –6.55 | –5.79 | –6.90 | –11.23 | –3.78 | –2.34 | 0.57 | 1.53 | –0.51 | 0.25 | 1.49 | –0.31 | 1.44 | 1.55 | 11.66 | 3.68 |
| Rb | 14 | 25 | 13 | 7 | 5 | 20 | 71 | 12.82 | 40 | 251 | 121 | 133 | 87 | 157 | 45 | 233 | 90 |
| 8 | | | | | | | | | | | | | | | | | |
| Sr | 309 | 306 | 272 | 302 | 253 | 168 | 488 | 255 | 330 | 210 | 330 | 583 | 530 | 1133 | 172 | 423 | 242 |
| Ba | 234 | 596 | 291 | 169 | 114 | 185 | 1175 | 849 | 2277 | 1131 | 1469 | 1710 | 2036 | 2675 | 1182 | 1262 | 185 |
| Y | 30 | 31 | 35 | 21 | 24 | 36 | 46 | 10 | 2 | 6 | 11 | 18 | 4 | 25 | 43 | 71 | 90 |
| Zr | 146 | 244 | 225 | 110 | 101 | 148 | 376 | 106 | 37 | 187 | 711 | 353 | 168 | 304 | 314 | 383 | 746 |
| Hf | 3.8 | 5.8 | 5.8 | 2.8 | 2.7 | 3.9 | 8.4 | 2.6 | 0.9 | 5.2 | 18.7 | 9.2 | 4.0 | 7.6 | 8.3 | 10.3 | 21.7 |
| Nb | 8.3 | 17.2 | 21.2 | 9.9 | 5.0 | 8.2 | 71.4 | 3.6 | 3.0 | 7.7 | 8.4 | 6.9 | 8.1 | 27.7 | 15.7 | 19.1 | 12.7 |
| Ta | 0.92 | 0.97 | 1.55 | 0.68 | 0.18 | 0.44 | 5.89 | 0.10 | 0.04 | 0.26 | 0.26 | 0.26 | 0.41 | 1.91 | 0.91 | 1.21 | 0.56 |
| Zn | 107 | 126 | 97 | 84 | 70 | 111 | 72 | 44 | 11 | 30 | 51 | 33 | 8 | 132 | 78 | 114 | 75 |
| Cu | 63 | 38 | 125 | 92 | 34 | 45 | 39 | 5 | 2 | 26 | –1 | 14 | 10 | 10 | 27 | 72 | 1 |
| V | 311 | 303 | 238 | 304 | 266 | 286 | 187 | 34 | 9 | 30 | 36 | 43 | 27 | 168 | 107 | 105 | 69 |
| Ni | 62 | 38 | 83 | 67 | 61 | 49 | 10 | 2 | <1 | 7 | 3 | 8 | <1 | 7 | 23 | 25 | 10 |
| Cr | 99 | 67 | 57 | 56 | 197 | 114 | 16 | 5 | <0.5 | 15 | 3 | 21 | 2 | 11 | 91 | 73 | 113 |
| Co | 52.5 | 55.0 | 49.8 | 59.4 | 42.5 | 53.5 | 25.2 | 5.0 | 1.4 | 7.5 | 6.6 | 10.2 | 3.4 | 24.3 | 20.5 | 18.0 | 11.2 |
| Sc | 32.5 | 31.6 | 27.0 | 27.7 | 44.9 | 47.7 | 20.5 | 6.8 | 0.3 | 3.8 | 3.8 | 6.4 | 1.2 | 10.3 | 22.3 | 23.4 | 19.7 |
| La | 13.9 | 23.0 | 26.3 | 9.9 | 15.1 | 27.5 | 89.7 | 30.4 | 38.5 | 34.5 | 47.2 | 53.7 | 71.9 | 46.4 | 69.2 | 60.4 | 73.7 |
| Ce | 32.5 | 52.9 | 55.5 | 23.0 | 34.4 | 62.7 | 174.9 | 53.1 | 47.8 | 61.0 | 66.5 | 88.0 | 101.6 | 99.8 | 127.4 | 125.8 | 140.4 |
| Pr | 4.36 | 5.88 | 7.82 | 2.91 | 3.59 | 7.30 | 18.15 | 5.56 | 3.42 | 6.06 | 7.41 | 9.70 | 7.87 | 13.23 | 12.73 | 15.57 | 14.36 |
| Nd | 20.6 | 27.4 | 32.5 | 13.4 | 15.7 | 29.4 | 65.1 | 20.0 | 10.6 | 22.7 | 24.1 | 35.5 | 21.9 | 54.3 | 45.4 | 56.0 | 51.4 |
| Sm | 5.01 | 6.17 | 7.75 | 3.49 | 3.42 | 6.45 | 10.69 | 3.16 | 1.33 | 3.48 | 3.93 | 5.91 | 2.26 | 11.16 | 7.77 | 11.30 | 8.41 |
| Eu | 1.71 | 2.51 | 2.67 | 1.40 | 1.36 | 1.59 | 2.78 | 0.91 | 1.87 | 1.36 | 2.01 | 1.74 | 1.08 | 3.81 | 2.10 | 1.68 | 2.08 |
| Gd | 5.36 | 7.03 | 7.50 | 4.02 | 4.14 | 6.56 | 9.35 | 2.57 | 0.71 | 2.61 | 3.21 | 4.97 | 1.34 | 9.07 | 7.53 | 10.66 | 10.57 |
| Tb | 0.92 | 1.16 | 1.27 | 0.72 | 0.75 | 1.17 | 1.52 | 0.31 | 0.12 | 0.31 | 0.39 | 0.68 | 0.20 | 1.21 | 1.32 | 2.07 | 2.08 |
| Dy | 5.58 | 6.65 | 7.28 | 3.97 | 4.73 | 6.70 | 8.40 | 1.70 | 0.53 | 1.39 | 1.98 | 3.40 | 0.92 | 5.83 | 7.69 | 12.79 | 13.38 |
| Ho | 1.08 | 1.33 | 1.39 | 0.78 | 1.00 | 1.38 | 1.70 | 0.34 | 0.09 | 0.24 | 0.39 | 0.65 | 0.17 | 0.97 | 1.57 | 2.67 | 2.96 |
| Er | 2.94 | 3.65 | 3.73 | 2.25 | 2.89 | 4.07 | 5.00 | 1.06 | 0.26 | 0.67 | 1.09 | 1.88 | 0.53 | 2.24 | 4.75 | 7.86 | 8.80 |
| Tm | 0.437 | 0.501 | 0.486 | 0.325 | 0.432 | 0.627 | 0.758 | 0.170 | 0.034 | 0.080 | 0.170 | 0.245 | 0.058 | 0.258 | 0.735 | 1.133 | |
| 1.390 | | | | | | | | | | | | | | | | | |
| Yb | 2.66 | 3.30 | 3.02 | 1.96 | 2.83 | 3.91 | 4.70 | 1.09 | 0.20 | 0.61 | 1.28 | 1.57 | 0.45 | 1.49 | 4.65 | 7.50 | 8.52 |
| Lu | 0.397 | 0.476 | 0.476 | 0.293 | 0.435 | 0.597 | 0.688 | 0.174 | 0.027 | 0.110 | 0.228 | 0.246 | 0.067 | 0.209 | 0.712 | 1.099 | |
| 1.330 | | | | | | | | | | | | | | | | | |
| U | 0.43 | 0.26 | 0.53 | 0.30 | 0.32 | 0.53 | 1.13 | 0.10 | 0.19 | 0.42 | 1.03 | 0.56 | 0.35 | 0.14 | 1.01 | 2.10 | 0.43 |
| Th | 1.61 | 2.00 | 2.03 | 1.02 | 3.16 | 2.73 | 6.45 | 0.44 | 2.55 | 1.45 | 3.82 | 4.35 | 42.92 | 0.91 | 24.85 | 14.52 | 4.44 |

*Note:* Oxide values are in wt %; trace element values are ppm. Abbreviation: LOI—loss on ignition.

*data from Carrigan et al., 2003; † normative corundum; negative C values reflect deficiency in $Al_2O_3$ relative to $CaO+Na_2O+K_2O$ after forming normative apatite

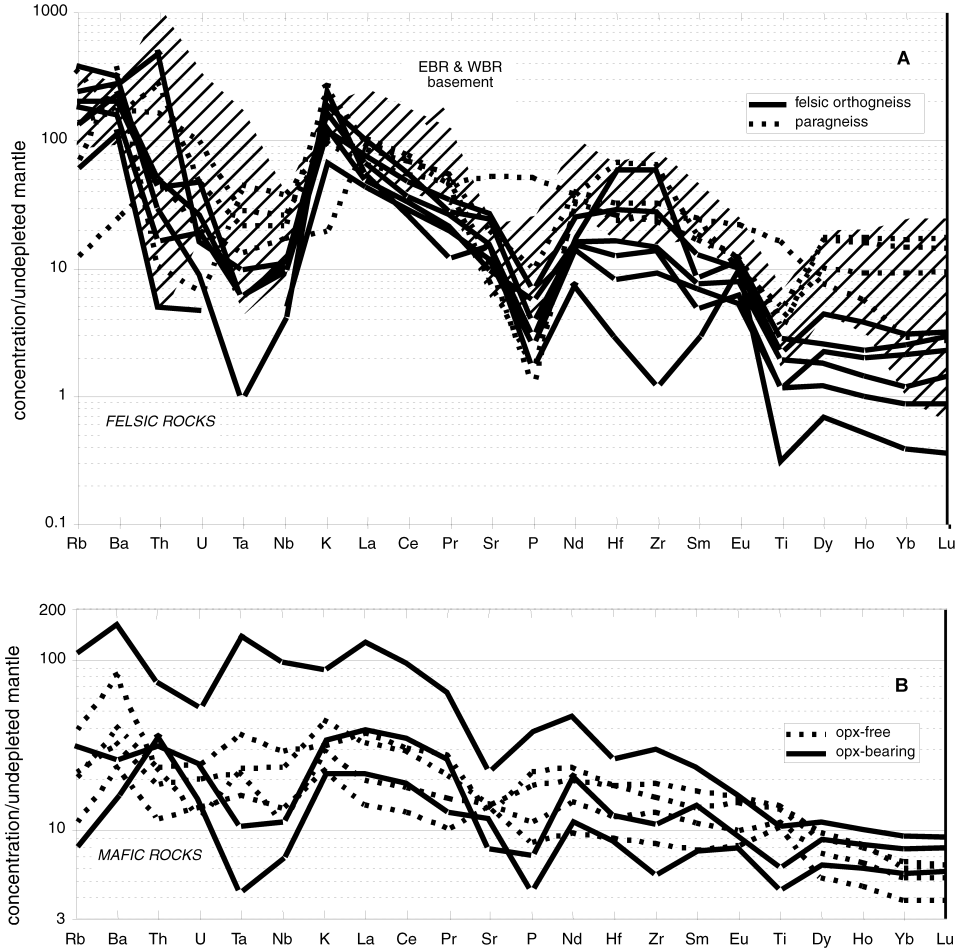


Figure 5. Elemental concentrations normalized to primitive mantle. Normalization values and element sequence are from Sun and McDonough (1989). The field of Eastern Blue Ridge (EBR) and Western Blue Ridge (WBR) basement is from Carrigan (2000) and Carrigan et al. (2003).

stone that was enriched in zircon by sedimentary processes. However, it lacks any other evidence for compositional effects induced by weathering or the mechanical concentration of grains in a sandstone. It has only 0.3 wt % normative corundum, is rich in Sr, and not unusually quartz-rich. The high Zr could reflect either origin as a relatively high-*T* rhyolite—the calculated zircon saturation temperature for RM30 is 937 °C—or as a cumulate-rich intrusive rock, consistent with its high Sr and positive Eu anomaly.

Elementally based protolith interpretations suggest that meta-igneous rocks may have been bimodal, with no analyzed samples between 53 and 70 wt % $SiO_2$. The felsic orthogneisses range from K-poor to highly potassic (2.3 to 8.5 wt % $K_2O$) and have distinctive rare-earth-element (REE) patterns, with common positive Eu anomalies and low heavy REE (HREE) (Fig. 4, A). Moderate enrichment of incompatible elements with large negative high-field-strength-element (HFSE) anomalies is evident on primitive mantle-normalized spider plots (Fig. 5, A). RM1, the 1.8-Ga felsic sample of Carrigan et al. (2003), is more silicic but much lower in K and Rb than the samples investigated in this study. The paragneisses have no or negative Eu anomalies and much higher HREE contents than do the felsic orthogneisses. Mafic samples, with 45 to 52 wt % $SiO_2$, are relatively rich in $K_2O$ (0.5 to 1.4, except for MBCL5A, with 2.7 wt %) and other incompatible elements compared with average basalts. The mafic rocks are mildly enriched in light REE (LREE) relative to HREE; MBCL5A is especially LREE rich (Fig. 4, B). All mafic samples have broadly similar incompatible element enrichment patterns. There are, however, subtle but important differences (Figs. 5, B and 6 and the following discussion).

The U concentrations are for the most part low in analyzed samples (<~1 ppm) and Th/U ratios are high, as is typical of rocks that have undergone granulite-facies metamorphism (e.g., Zartman and Doe, 1981). The mean Th/U ratios of paragneisses (12), felsic orthogneisses (21), and opx-bearing mafic gneisses (6.2) are well above the global average of ~4. In contrast, the average opx-free mafic rock has a ratio of 4.4, possibly because these samples did not experience the highest-grade event.

The MHT samples are compared with analyses of Eastern Blue Ridge and Western Blue Ridge basement (Carrigan, 2000)

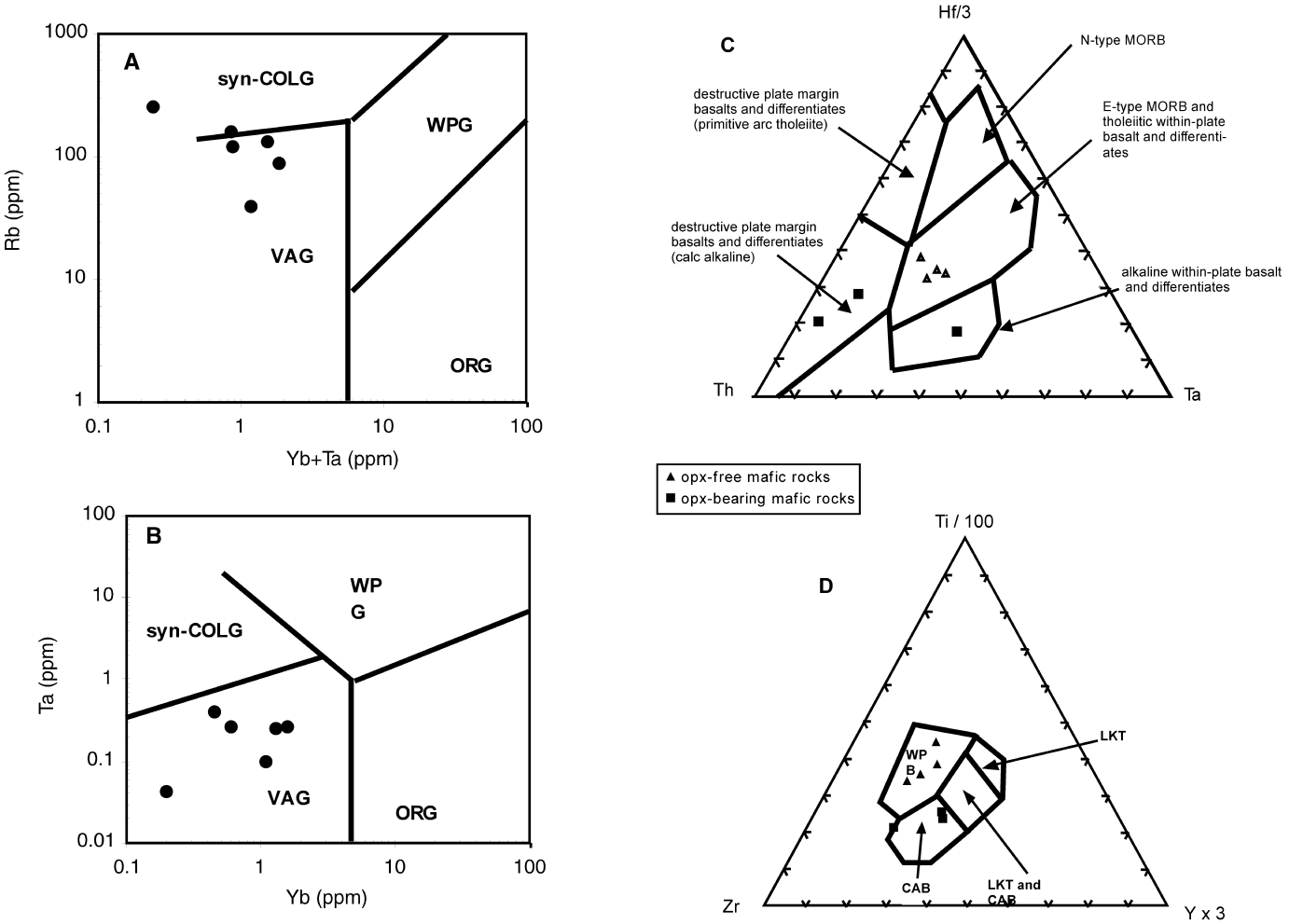


Figure 6. Tectonic discrimination diagrams. Felsic orthogneisses are plotted in 6A and 6B, mafic samples in 6C and 6D. (A) Rb versus Yb + Ta diagram of Pearce et al. (1984). ORG—ocean ridge granite; SYN COLG—syn-collisional granite; VAG—volcanic-arc granite; WPG—within-plate granite. (B) Ta versus Yb diagram of Pearce et al. (1984). Symbols as in panel A. (C) Hf-Th-Ta diagram of Wood (1980). MORB—Mid-oceanic ridge basalt. (D) Ti-Zr-Y diagram of Pearce and Cann (1973). LKT—Low-K tholeiite; WPT—within-plate tholeiite; CAB—calc-alkaline basalt.

in Figures 2, 4, and 5. MHT felsic orthogneisses are distinct from samples of basement from elsewhere in the southern Blue Ridge. The Eastern Blue Ridge and Western Blue Ridge basement gneisses have a wider range of $SiO_2$, higher REE concentrations (especially HREE), negative Eu anomalies, and somewhat higher incompatible element enrichments.

In standard tectonic discrimination diagrams (Fig. 6), the felsic orthogneisses generally plot together within the fields for arc-related granites, suggesting that they were either generated in an arc setting or derived from arc-generated crust. All four opx-free mafic samples plot as "within-plate basalts." The three opx-bearing mafic rocks plot within the calc-alkaline or arc basalts field on the Ti-Zr-Y diagram of Pearce and Cann (1973); on the Hf-Th-Ta diagram of Wood (1980), two plot as arc basalts, but the incompatible-element-rich rock, MBCL5A, plots alone in the field of alkaline within-plate basalts.

The Sm-Nd isotopic systematics of MHT samples document the antiquity of the crust that they represent (Table 2; Fig. 7). Two felsic orthogneisses, two opx-bearing mafic gneisses, and a paragneiss have Sm-Nd depleted mantle model ages (DePaolo, 1981) of ca. 1.7 to 2.3 Ga, and their calculated $\varepsilon_{Nd}$ values during Grenville time were –2 to –7, considerably lower than those of basement granitic gneisses of the Eastern Blue Ridge and Western Blue Ridge at the same time (approximately –1 to +3). Two opx-free mafic samples have much higher $\varepsilon_{Nd}$ (calculated as approximately +4 and +5 during Grenville time). Their values at 730 Ma (+1 and +3) are essentially identical to those calculated from whole-rock data for Bakersville dikes (Goldberg et al., 1986) (Fig. 7).

Calculated $^{87}Sr/^{86}Sr$ ratios of the felsic orthogneiss and paragneiss samples during Grenville time (1.0–1.2 Ga) range from 0.706 to 0.714. These high ratios, like the low Nd ratios,

**TABLE 2. WHOLE-ROCK ISOTOPIC DATA**

| | Mafic, opx-free | | Mafic, opx-bearing | | Felsic gneiss | | Paragneiss |
|---|---|---|---|---|---|---|---|
| | RM2 | RM2X | RM24 | RM30C | RM1 | RM15 | RM-CLG |
| Approximate age (Ga)* | 0.73 | 0.73 | 1.2 | 1.2 | 1.8 | 1.2 | 1.2 |
| Rb (ppm) | 12.25 | 22.43 | 4.95 | 20.83 | 39.06 | 258.37 | 7.81 |
| Sr (ppm) | 310.1 | 304.9 | 267.9 | 147.7 | 253.6 | 346.0 | 249.6 |
| $^{87}Rb/^{86}Sr$† | 0.114 | 0.213 | 0.054 | 0.4086 | 0.446 | 2.168 | 0.091 |
| $^{87}Sr/^{86}Sr_{measured}$ | 0.704732 | 0.706333 | 0.707354 | 0.719332 | 0.718556 | 0.742263 | 0.715261 |
| s??? $^{87}Sr/^{86}Sr$ (%) | 0.0008 | 0.0010 | 0.0008 | 0.0008 | 0.0007 | 0.0009 | 0.0008 |
| $^{87}Sr/^{86}Sr_{initial}$ | 0.70354 | 0.70411 | 0.70643 | 0.71231 | 0.70701 | 0.70500 | 0.71370 |
| $^{87}Sr/^{86}Sr_{1.15}$‡ | 0.70286 | 0.70282 | 0.70646 | 0.71260 | 0.71121 | 0.70657 | 0.71376 |
| Nd (ppm) | 5.01 | 6.38 | 3.68 | 8.40 | 2.85 | 1.48 | 7.69 |
| Sm (ppm) | 19.28 | 26.99 | 16.18 | 37.31 | 19.00 | 11.01 | 48.04 |
| $^{147}Sm/^{144}Nd$† | 0.1607 | 0.1462 | 0.1407 | 0.1394 | 0.0929 | 0.0831 | 0.0990 |
| $^{143}Nd/^{144}Nd_{measured}$ | 0.512625 | 0.512443 | 0.512112 | 0.511915 | 0.511489 | 0.511625 | 0.511637 |
| s.e. $^{143}Nd/^{144}Nd$ (%) | 0.0004 | 0.0009 | 0.0008 | 0.0007 | 0.0012 | 0.0005 | 0.0008 |
| $\varepsilon_{Nd,present\ day}$ | –0.25 | –3.80 | –10.26 | –14.10 | –22.41 | –19.76 | –19.53 |
| $^{143}Nd/^{144}Nd_{initial}$ | 0.511856 | 0.511743 | 0.511003 | 0.510817 | 0.510389 | 0.510970 | 0.510857 |
| $\varepsilon_{Nd,initial}$ | 3.11 | 0.91 | –1.66 | –5.31 | 1.57 | –2.31 | –4.52 |
| $^{143}Nd/^{144}Nd_{1.15}$‡ | 0.511412 | 0.511339 | 0.511050 | 0.510863 | 0.510788 | 0.510998 | 0.510890 |
| $\varepsilon_{Nd1150}$ | 5.06 | 3.64 | –2.02 | –5.68 | –7.15 | –3.04 | –5.15 |
| $T_{DM}$ (Ga) | 1.20 | 1.35 | 1.94 | 2.32 | 1.96 | 1.65 | 1.82 |

*Note:* Data for samples RM2, RM1, and RM-CLG are from Carrigan et al (2003). Model age $T_{DM}$ is calculated according to DePaolo (1981).
*For calculation of initial ratio.
†Sm/Nd and Rb/Sr uncertainties are estimated to be <1% (2σ).
‡Calculated at 1.15 Ga for comparison.

indicate that they were derived from much older crust. The opx-bearing mafic samples have calculated Grenville ratios of >0.706, whereas the two opx-free mafic samples both have a Grenville ratio of 0.703. Recalculated at 730 Ma, the age of Bakersville dikes (and the age of CAR 1501—see the Geochronology section), both opx-free samples yield ratios of 0.7035 and 0.7041. These ratios are similar to the initial ratio of 0.7044 obtained by Goldberg et al. (1986) from a whole-rock isochron for Bakersville samples. Open-system behavior during granulite-facies metamorphism would tend to lower Rb/Sr ratios and possibly increase $^{87}Sr/^{86}Sr$ ratios through interaction with nearby, more radiogenic Sr reservoirs. Thus, the calculated ratios are probably maxima, but the distinction between opx-bearing and opx-free mafic rocks appears real, as does the similarity of the opx-free samples to Bakersville dikes.

## GEOCHRONOLOGY

As noted previously, Monrad and Gulley (1983), Fullagar and Gulley (1999), and Carrigan et al. (2003) have all reported ages of ca. 1.8 Ga for Carvers Gap orthogneiss from Roan Mountain. Fullagar and Gulley (1999) also obtained an upper-intercept age of 1.4 Ga for another Carvers Gap sample. Carrigan et al. (2003) analyzed zircons from four other Roan Mountain samples by ion microprobe, two of Carvers Gap gneiss and two of Cloudland paragneiss. The orthogneiss samples yielded imprecise ages of ca. 1.6 Ga and 1.2 Ga, interpreted as the time of magmatic crystallization. Cores of detrital grains from Cloudland gneiss gave nearly concordant ages ranging from ~1.0 to 1.85 Ga. The youngest ages approach and in some cases are younger than the age of ubiquitous metamorphic rims (ca. 1.03 Ga) and therefore probably reflect Pb loss. However, the abundant concordant ages strongly indicate a range of Mesoproterozoic to Paleoproterozoic detrital ages. Fullagar et al. (1979) reported a whole-rock Rb-Sr age of 1183 ± 65 Ma for granitic gneiss from near Mars Hill.

Sites for SHRIMP U-Pb analysis of zircons from the seven samples investigated for this study were selected and interpreted in part on the basis of zoning evident in cathodoluminescence images. We interpret zoning based on criteria described in Miller et al. (1992, 1998), Hanchar and Miller (1993), and references therein. Almost all grains are strikingly zoned, with bright (less commonly, dark), weakly zoned or unzoned rims that we interpret to be metamorphic and having one or more distinct interior zones. Some grains have zoning that suggests two discrete metamorphic overgrowths, and others have distinct cores with magmatic overgrowths (characterized by euhedral, in some cases oscillatory zoning), all surrounded by a metamorphic rim.

In the following discussion, we briefly describe the zoning (Fig. 8) and U-Pb data (Table 3; Fig. 9) for zircons from each of the samples. In general, metamorphic data are concordant or nearly so, but imprecise owing to low U and Pb concentrations, whereas magmatic and premagmatic data for most samples are discordant. This discordance may in small part reflect beam overlap into two distinct age zones, but the fact that analyses commonly define discordia with young lower intercepts that do

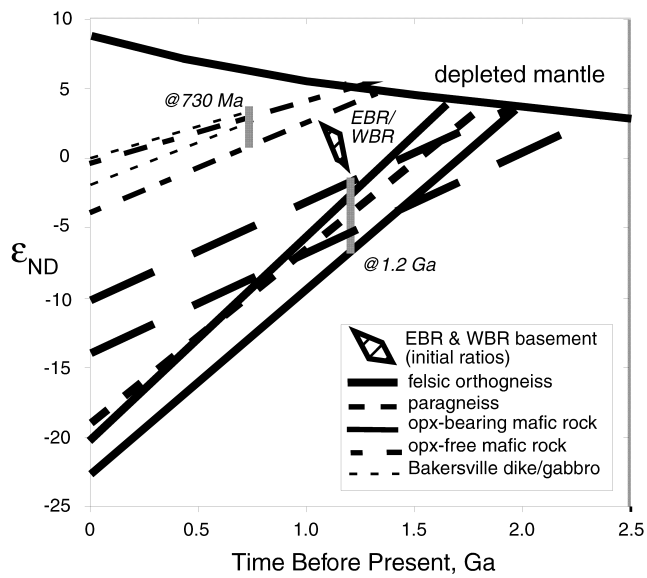


Figure 7. Calculated Nd isotopic evolution of samples analyzed in this study, plus two whole-rock analyses of Bakersville rocks by Goldberg and Dallmeyer (1997). Depleted mantle curve is from DePaolo (1981). Eastern Blue Ridge/Western Blue Ridge basement field from Carrigan (2000) and Carrigan et al. (2003). Gray bars at 730 Ma and 1.2 Ga show ranges of initial values of opx-free mafic rocks + Bakersville dikes and of gabbros and other Mars Hill samples, respectively.

not correspond to ages of any identifiable zones—in several cases, zero-age lower intercepts—indicates that most discordance is a result of Pb loss. The greater discordance of U-rich magmatic zones than of U-poor metamorphic zones is consistent with discordance through Pb loss. There is essentially no correlation between Th/U ratio and zone type (Table 3).

For the most abundant age populations, which we interpret to reflect magmatic crystallization or possibly detrital reworking of a slightly older igneous source, we have estimated age in two ways. First, we have pooled the $^{207}Pb/^{206}Pb$ ages of the more concordant points, and second, we have determined upper intercepts of discordia for those samples for which the data fit well on a regression. For those samples that define a discordia, the upper intercept is invariably within the error of the pooled $^{207}Pb/^{206}Pb$ age. In fact, five samples (all but two) yield ages within error of one another at 1.20 Ga. In Figure 9, both discordia (if defined by the data) and a constant $^{207}Pb/^{206}Pb$ age reference line (from the origin through the approximate magmatic age) are shown. Lower intercepts of the discordia are either near zero or imprecisely defined Paleozoic ages.

The less precise metamorphic ages are estimated in most cases by pooling $^{207}Pb/^{206}Pb$ ages; in some cases, the data can be fit to a discordia. Although the dominant metamorphic age is clearly near 1.0 Ga, there is some evidence that there may be a second, older metamorphic population, but there are too few points to define this age well. Older, apparently detrital and inherited cores are mostly discordant, and we take individual $^{207}Pb/^{206}Pb$ ages as the best estimates for the ages of these zones.

All stated age uncertainties in the text and Table 3 are $\pm 2\sigma$; intercept errors in Figure 9 are also $2\sigma$, but error ellipses on concordia plots are $1\sigma$ for clarity.

### RM21—Felsic Orthogneiss

Zircons in RM21 have simple, concentric internal zones; in some cases, euhedral and, rarely, oscillatory (Fig. 8, A). Based on zone morphology alone, it is difficult to distinguish magmatic from inherited portions with certainty, but rare truncated zoned fragments in the centers are the best candidates for inherited cores. Most grains have thick, bright overgrowths that we interpret to be metamorphic; in some cases, these form the rims, but in others, they are surrounded by a thin, darker rim zone.

Five discordant interior points that we interpret to be magmatic fall on a zero-lower-intercept discordia with an upper intercept of 1198 ± 26 Ma (mean square of weighted deviations [MSWD], 0.30) (Fig. 9, A). The four most concordant points yield an identical $^{207}Pb/^{206}Pb$ age (MSWD, 0.40) (Fig. 9, A). Two analyses from cores have discordant $^{207}Pb/^{206}Pb$ ages of 1276 and1538 Ma. The $^{207}Pb/^{206}Pb$ ages of nine points from rims and probable metamorphic interiors average 1026 ± 19 Ma (MSWD, 1.02).

### RM38—Felsic, Mylonitic Orthogneiss

Zircons from RM38 (Fig. 8, B) are well formed and prismatic, with euhedral and locally oscillatory zones that we interpret to be magmatic. Dark cores in the magmatic portions are rare. All grains have thin to thick bright, rounded rims that we interpret to be metamorphic, and some have slightly less bright zones inside the bright rims that appear to mark earlier metamorphic growth.

Ten analyses from zones interpreted as magmatic or possibly magmatic define a discordia with an upper intercept of 1200 ± 26 Ma and a lower intercept of 383 ± 110 Ma (MSWD, 1.13) (Fig. 9, B). The five most concordant points have a mean $^{207}Pb/^{206}Pb$ age of 1185 ± 36 Ma (MSWD, 2.2); the slightly younger age and higher MSWD reflect the fact that these points actually lie on the well-defined discordia defined by all ten magmatic points, which has a nonzero lower intercept. One dark unzoned (presumably inherited) core yielded a $^{207}Pb/^{206}Pb$ age of 1511 ± 69 Ma.

### MBCL4—Felsic Orthogneiss

Zircons from MBCL4 have very well-defined euhedral, oscillatory magmatic zoning and thin to thick, bright metamorphic rims (Fig. 8, C). No cores are evident. Eleven points from magmatic zones define a discordia with an upper intercept of 1257 ± 26 Ma and a lower intercept of 540 ± 280 (MSWD, 0.35) (Fig. 9, C). The ten most concordant points have a mean

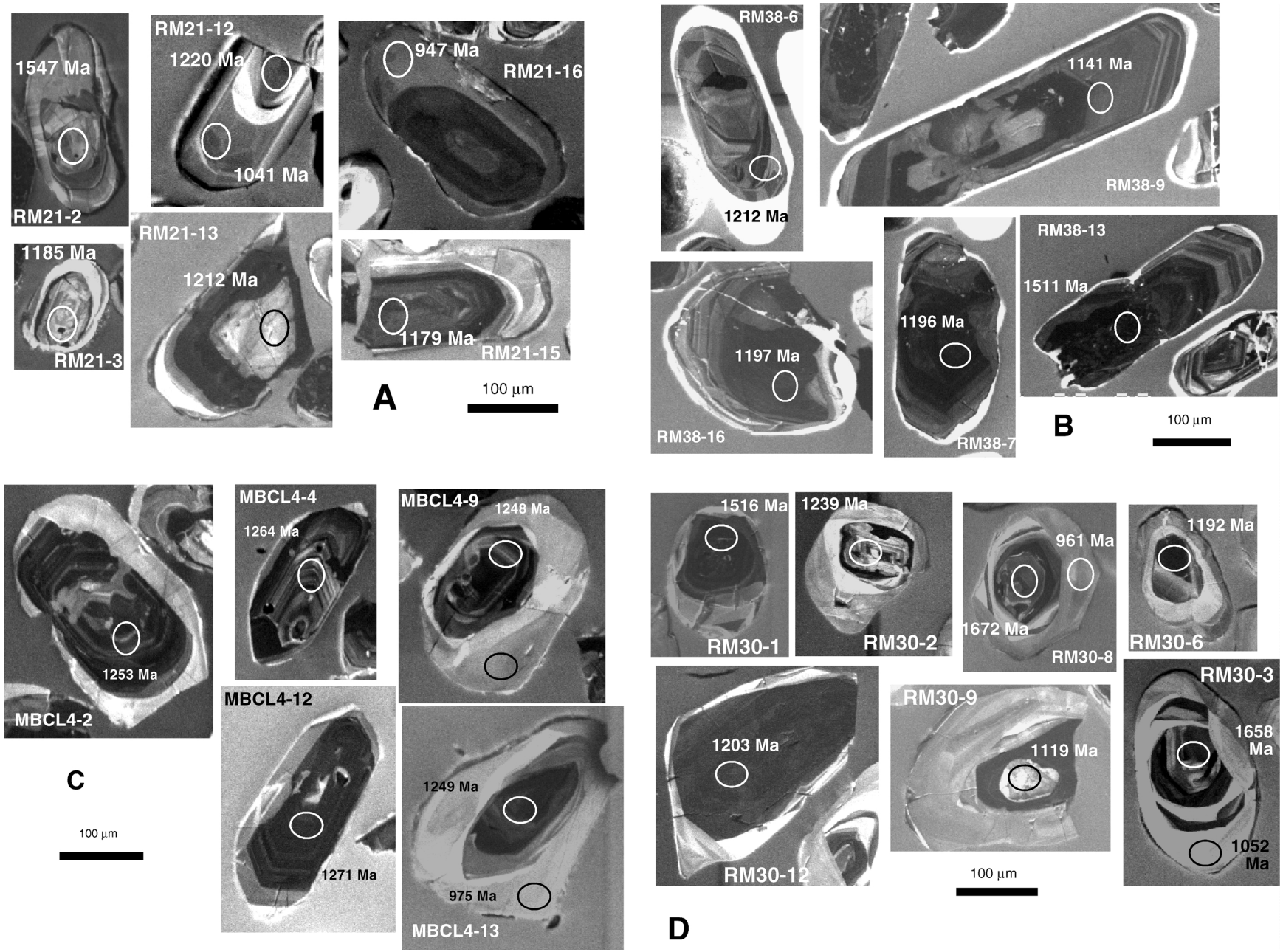
1547 Ma
RM21-2
RM21-12
1220 Ma
1041 Ma
947 Ma
RM21-16
1185 Ma
RM21-3
RM21-13
1212 Ma
1179 Ma
RM21-15
A
100 µm
RM38-6
1212 Ma
1141 Ma
RM38-9
1197 Ma
RM38-16
1196 Ma
RM38-7
RM38-13
1511 Ma
B
100 µm
1253 Ma
MBCL4-2
MBCL4-4
1264 Ma
MBCL4-9
1248 Ma
C
100 µm
MBCL4-12
1271 Ma
1249 Ma
975 Ma
MBCL4-13
1516 Ma
RM30-1
1239 Ma
RM30-2
961 Ma
1672 Ma
RM30-8
1192 Ma
RM30-6
1203 Ma
RM30-12
RM30-9
1119 Ma
100 µm
RM30-3
1658 Ma
1052 Ma
D

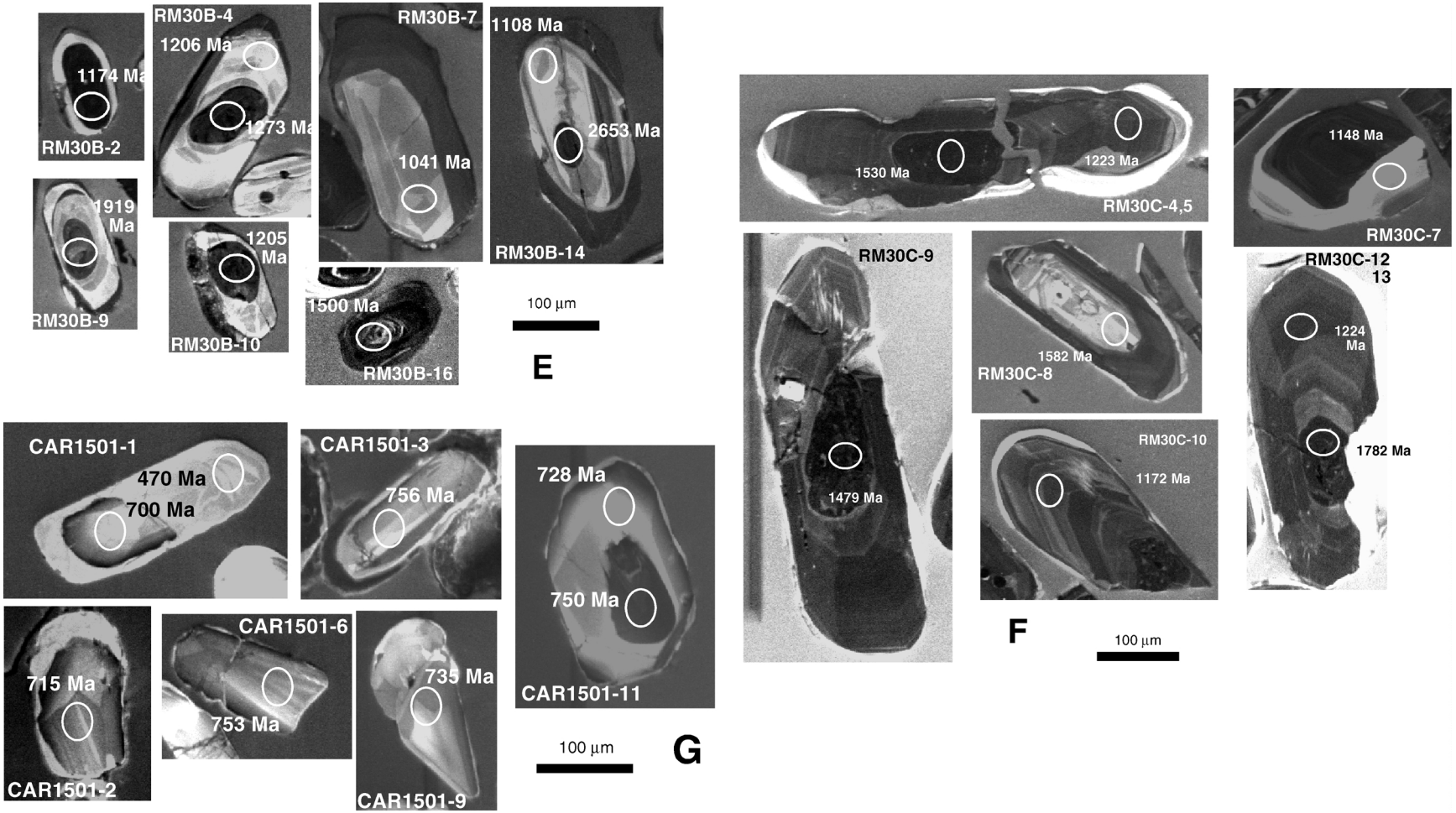


Figure 8. Cathodoluminescence images of representative Mars Hill zircons that were analyzed. Ages are $^{207}Pb/^{206}Pb$, except for CAR 1501 ($^{206}Pb/^{238}U$); ellipses show approximate spot size and location. Labels denote sample and zircon analysis numbers (see Table 3).

## TABLE 3. U-PB ZIRCON DATA

| Analysis number | Zone type* | Common. $^{206}Pb$ (%) | U (ppm) | Th (ppm) | $^{232}Th/^{238}U$ | $^{206}Pb/^{238}U$ age† | 2σ error | $^{207}Pb/^{206}Pb$ age§ | 2σ error | Total $^{238}U/^{206}Pb$ | Error (%) | Total $^{207}Pb/^{206}Pb$ | Error (%) | $^{207}Pb\#/^{235}U$ | Error (%) | $^{206}Pb\#/^{238}U$ | Error (%) | Error correlation |
|---|---|---|---|---|---|---|---|---|---|---|---|---|---|---|---|---|---|---|
| RM21-1 | DUI | 0.02 | 2180 | 376 | 0.18 | 1054 | 24 | 1206 | 39 | 5.59 | 1.17 | 0.0805 | 0.98 | 1.983 | 1.53 | 0.179 | 1.17 | 0.76 |
| RM21-2 | GZC | 0.15 | 188 | 140 | 0.77 | 1316 | 41 | 1547 | 154 | 4.35 | 1.55 | 0.0972 | 3.93 | 3.033 | 4.38 | 0.229 | 1.56 | 0.36 |
| RM21-3 | GEC | –0.02 | 349 | 123 | 0.36 | 1162 | 31 | 1185 | 67 | 5.06 | 1.37 | 0.0794 | 1.70 | 2.169 | 2.18 | 0.198 | 1.37 | 0.63 |
| RM21-4 | DZC | 0.02 | 2050 | 119 | 0.06 | 1009 | 23 | 1034 | 31 | 5.90 | 1.16 | 0.0739 | 0.75 | 1.723 | 1.39 | 0.170 | 1.16 | 0.84 |
| RM21-5 | BUR | –0.08 | 87 | 182 | 2.17 | 988 | 36 | 1014 | 159 | 6.04 | 1.86 | 0.0723 | 3.96 | 1.669 | 4.34 | 0.166 | 1.86 | 0.43 |
| RM21-6 | BUR | –0.07 | 88 | 172 | 2.02 | 1068 | 38 | 1100 | 145 | 5.55 | 1.81 | 0.0756 | 3.67 | 1.895 | 4.06 | 0.180 | 1.81 | 0.45 |
| RM21-8 | DUC | 0.03 | 3004 | 278 | 0.10 | 929 | 21 | 1022 | 29 | 6.42 | 1.18 | 0.0736 | 0.70 | 1.573 | 1.38 | 0.156 | 1.18 | 0.86 |
| RM21-9 | GEC | 0.00 | 2237 | 334 | 0.15 | 1149 | 26 | 1276 | 39 | 5.10 | 1.16 | 0.0832 | 1.00 | 2.253 | 1.53 | 0.196 | 1.16 | 0.76 |
| RM21-10 | BUR | –0.07 | 108 | 209 | 2.01 | 997 | 34 | 1016 | 143 | 5.98 | 1.75 | 0.0725 | 3.56 | 1.687 | 3.94 | 0.167 | 1.75 | 0.44 |
| RM21-11 | BUI | –0.10 | 68 | 164 | 2.47 | 970 | 38 | 1103 | 170 | 6.13 | 2.01 | 0.0755 | 4.29 | 1.719 | 4.69 | 0.163 | 2.01 | 0.43 |
| RM21-12 | GZR | 0.21 | 180 | 345 | 1.98 | 1034 | 30 | 1041 | 122 | 5.73 | 1.49 | 0.0758 | 2.51 | 1.775 | 3.37 | 0.174 | 1.50 | 0.44 |
| RM21-12B | GUC | –0.02 | 299 | 83 | 0.29 | 1031 | 28 | 1220 | 72 | 5.72 | 1.40 | 0.0808 | 1.83 | 1.952 | 2.30 | 0.175 | 1.40 | 0.61 |
| RM21-13 | BZC | –0.04 | 150 | 133 | 0.92 | 971 | 30 | 1212 | 164 | 6.09 | 1.54 | 0.0803 | 4.18 | 1.826 | 4.43 | 0.164 | 1.54 | 0.35 |
| RM21-14 | BUR | 0.56 | 66 | 150 | 2.33 | 979 | 38 | 765 | 278 | 6.12 | 1.95 | 0.0693 | 4.30 | 1.451 | 6.89 | 0.163 | 1.99 | 0.29 |
| RM21-15 | DEI | –0.01 | 501 | 473 | 0.98 | 1141 | 28 | 1179 | 54 | 5.16 | 1.29 | 0.0792 | 1.38 | 2.121 | 1.88 | 0.194 | 1.29 | 0.68 |
| RM21-16 | GUR | –0.03 | 176 | 262 | 1.54 | 984 | 30 | 947 | 104 | 6.07 | 1.56 | 0.0704 | 2.54 | 1.604 | 2.98 | 0.165 | 1.56 | 0.53 |
| RM38-1 | DUC | 0.00 | 3183 | 157 | 0.05 | 937 | 21 | 1134 | 26 | 6.34 | 1.15 | 0.0775 | 0.65 | 1.687 | 1.32 | 0.158 | 1.15 | 0.87 |
| RM38-6 | GEI | 0.06 | 582 | 195 | 0.35 | 1143 | 28 | 1212 | 68 | 5.13 | 1.25 | 0.0811 | 1.68 | 2.163 | 2.14 | 0.195 | 1.25 | 0.58 |
| RM38-7 | DUI | 0.03 | 2770 | 578 | 0.22 | 1144 | 25 | 1196 | 25 | 5.14 | 1.15 | 0.0802 | 0.61 | 2.146 | 1.31 | 0.195 | 1.15 | 0.88 |
| RM38-8 | GUI | –0.03 | 307 | 135 | 0.46 | 776 | 22 | 1034 | 126 | 7.74 | 1.43 | 0.0735 | 3.13 | 1.314 | 3.43 | 0.129 | 1.43 | 0.42 |
| RM38-9 | GEI | 0.09 | 378 | 133 | 0.36 | 1126 | 29 | 1141 | 73 | 5.23 | 1.31 | 0.0786 | 1.71 | 2.048 | 2.27 | 0.191 | 1.31 | 0.58 |
| RM38-10 | DUC | 0.05 | 2357 | 132 | 0.06 | 1048 | 23 | 1149 | 41 | 5.64 | 1.15 | 0.0785 | 1.02 | 1.909 | 1.55 | 0.177 | 1.15 | 0.74 |
| RM38-11 | DZC | –0.01 | 904 | 143 | 0.16 | 925 | 22 | 1090 | 49 | 6.43 | 1.21 | 0.0757 | 1.23 | 1.625 | 1.73 | 0.155 | 1.21 | 0.70 |
| RM38-13 | DUC | 1.90 | 2011 | 292 | 0.15 | 1162 | 28 | 1511 | 139 | 4.88 | 1.15 | 0.1105 | 1.72 | 2.612 | 3.86 | 0.201 | 1.18 | 0.31 |
| RM38-15 | DUC | –0.01 | 888 | 238 | 0.28 | 1111 | 26 | 1132 | 45 | 5.31 | 1.20 | 0.0774 | 1.13 | 2.010 | 1.65 | 0.188 | 1.20 | 0.73 |
| RM38-16 | DUC | 0.00 | 1240 | 255 | 0.21 | 1164 | 27 | 1197 | 35 | 5.04 | 1.19 | 0.0800 | 0.89 | 2.187 | 1.49 | 0.198 | 1.19 | 0.80 |
| RM38-17 | GZI | 0.17 | 351 | 96 | 0.28 | 810 | 24 | 1020 | 109 | 7.40 | 1.49 | 0.0746 | 2.29 | 1.362 | 3.07 | 0.135 | 1.49 | 0.49 |
| MBCL-1 | DZC | 0.12 | 729 | 625 | 0.89 | 1012 | 24 | 1096 | 63 | 5.85 | 1.22 | 0.0770 | 1.24 | 1.788 | 2.00 | 0.171 | 1.22 | 0.61 |
| MBCL-2 | DEC | –0.01 | 469 | 329 | 0.73 | 1249 | 31 | 1253 | 56 | 4.68 | 1.26 | 0.0822 | 1.44 | 2.426 | 1.91 | 0.214 | 1.26 | 0.66 |
| MBCL-3 | BUR | –0.09 | 74 | 246 | 3.42 | 955 | 37 | 1485 | 145 | 6.11 | 1.93 | 0.0921 | 3.87 | 2.097 | 4.30 | 0.164 | 1.93 | 0.45 |
| MBCL-3B | DUC | 0.08 | 1136 | 64 | 0.06 | 1079 | 25 | 1199 | 59 | 5.45 | 1.20 | 0.0808 | 1.38 | 2.023 | 1.91 | 0.183 | 1.20 | 0.63 |
| MBCL-4 | GEC | 0.06 | 501 | 980 | 2.02 | 1276 | 41 | 1264 | 53 | 4.57 | 1.66 | 0.0833 | 1.28 | 2.496 | 2.14 | 0.219 | 1.66 | 0.78 |
| MBCL-5 | DUC | 0.00 | 1561 | 980 | 0.65 | 1275 | 28 | 1258 | 29 | 4.58 | 1.16 | 0.0825 | 0.74 | 2.487 | 1.37 | 0.219 | 1.16 | 0.84 |
| MBCL-6 | BZC | 0.97 | 96 | 114 | 1.24 | 1063 | 37 | 1203 | 270 | 5.49 | 1.75 | 0.0884 | 3.26 | 1.997 | 7.10 | 0.180 | 1.83 | 0.26 |
| MBCL-7 | DEI | 0.37 | 1063 | 461 | 0.45 | 1129 | 26 | 1240 | 65 | 5.18 | 1.19 | 0.0849 | 1.10 | 2.169 | 2.04 | 0.192 | 1.19 | 0.59 |
| MBCL-7B | GEI | 0.06 | 906 | 292 | 0.33 | 1140 | 27 | 1216 | 60 | 5.15 | 1.23 | 0.0813 | 1.49 | 2.162 | 1.96 | 0.194 | 1.23 | 0.63 |
| MBCL-8 | BUR | 1.73 | 63 | 206 | 3.39 | 1012 | 41 | 367 | 389 | 5.92 | 2.03 | 0.0678 | 4.70 | 1.233 | 8.88 | 0.166 | 2.06 | 0.23 |
| MBCL-9 | DEC | 0.08 | 374 | 721 | 1.99 | 1215 | 30 | 1248 | 66 | 4.81 | 1.29 | 0.0828 | 1.58 | 2.353 | 2.13 | 0.208 | 1.29 | 0.61 |
| MBCL-9B | BZR | –0.07 | 92 | 378 | 4.23 | 1012 | 36 | 925 | 155 | 5.91 | 1.80 | 0.0693 | 3.80 | 1.633 | 4.18 | 0.169 | 1.80 | 0.43 |
| MBCL-10 | BEC | 0.13 | 360 | 465 | 1.34 | 1210 | 31 | 1244 | 78 | 4.83 | 1.31 | 0.0830 | 1.71 | 2.336 | 2.38 | 0.207 | 1.32 | 0.55 |
| MBCL-11 | DZC | 0.11 | 646 | 671 | 1.07 | 1027 | 25 | 1029 | 70 | 5.78 | 1.27 | 0.0744 | 1.41 | 1.752 | 2.15 | 0.173 | 1.27 | 0.59 |
| MBCL-12 | DEC | 0.00 | 1301 | 662 | 0.53 | 1257 | 29 | 1271 | 32 | 4.64 | 1.18 | 0.0830 | 0.82 | 2.468 | 1.44 | 0.216 | 1.18 | 0.82 |
| MBCL-13A | DEC | 0.26 | 1529 | 944 | 0.64 | 972 | 24 | 1249 | 50 | 6.05 | 1.29 | 0.0844 | 0.87 | 1.866 | 1.82 | 0.165 | 1.29 | 0.71 |
| MBCL-13B | BUR | 0.73 | 117 | 275 | 2.42 | 1067 | 34 | 975 | 267 | 5.54 | 1.65 | 0.0777 | 3.10 | 1.770 | 6.76 | 0.179 | 1.72 | 0.25 |
| MBCL-15 | DZC | 0.00 | 1372 | 42 | 0.03 | 1172 | 27 | 1210 | 33 | 5.01 | 1.18 | 0.0805 | 0.83 | 2.217 | 1.44 | 0.200 | 1.18 | 0.82 |
| MBCL-16 | GEI | 0.09 | 361 | 394 | 1.13 | 1172 | 31 | 1202 | 69 | 5.00 | 1.35 | 0.0810 | 1.63 | 2.209 | 2.21 | 0.200 | 1.35 | 0.61 |
| RM30-1 | DZC | 0.38 | 1370 | 741 | 0.56 | 1241 | 29 | 1516 | 114 | 4.63 | 1.17 | 0.0977 | 2.75 | 2.802 | 3.25 | 0.215 | 1.17 | 0.36 |
| RM30-2 | BZC | –0.02 | 292 | 228 | 0.80 | 1136 | 31 | 1239 | 101 | 5.16 | 1.37 | 0.0815 | 2.57 | 2.183 | 2.91 | 0.194 | 1.37 | 0.47 |
| RM30-3A | GEC | –0.01 | 296 | 301 | 1.05 | 1657 | 45 | 1658 | 55 | 3.41 | 1.39 | 0.1017 | 1.50 | 4.116 | 2.04 | 0.293 | 1.39 | 0.68 |
| RM30-3B | BUR | –0.09 | 80 | 138 | 1.78 | 1068 | 41 | 1052 | 166 | 5.56 | 1.95 | 0.0736 | 4.16 | 1.847 | 4.55 | 0.180 | 1.95 | 0.43 |
| RM30-4 | BUR | –0.04 | 212 | 49 | 0.24 | 995 | 29 | 1062 | 105 | 5.97 | 1.50 | 0.0744 | 2.62 | 1.726 | 3.01 | 0.167 | 1.50 | 0.50 |
| RM30-5 | BZC | 0.26 | 754 | 84 | 0.11 | 1199 | 29 | 1320 | 58 | 4.85 | 1.26 | 0.0874 | 1.42 | 2.416 | 1.97 | 0.206 | 1.26 | 0.64 |
| RM30-6 | DZC | 0.03 | 1548 | 108 | 0.07 | 1125 | 26 | 1192 | 60 | 5.23 | 1.19 | 0.0800 | 1.50 | 2.105 | 1.92 | 0.191 | 1.19 | 0.62 |
| RM30-7 | DZC | 0.03 | 2435 | 1211 | 0.51 | 1273 | 33 | 1441 | 23 | 4.54 | 1.35 | 0.0910 | 0.59 | 2.754 | 1.48 | 0.220 | 1.35 | 0.91 |
| RM30-8 | GZC | –0.01 | 424 | 520 | 1.27 | 1676 | 42 | 1672 | 41 | 3.37 | 1.28 | 0.1026 | 1.10 | 4.201 | 1.69 | 0.297 | 1.28 | 0.76 |

| | | | | | | | | | | | | | | | | | | |
|---|---|---|---|---|---|---|---|---|---|---|---|---|---|---|---|---|---|---|
| RM30-8B | BUR | –0.05 | 164 | 178 | 1.12 | 1064 | 36 | 961 | 123 | 5.60 | 1.71 | 0.0707 | 3.02 | 1.753 | 3.45 | 0.179 | 1.71 | 0.50 |
| RM30-9 | BZC | 0.14 | 798 | 51 | 0.07 | 1018 | 26 | 1119 | 57 | 5.81 | 1.29 | 0.0781 | 1.37 | 1.822 | 1.92 | 0.172 | 1.29 | 0.67 |
| RM30-10 | DZI | 0.00 | 1571 | 254 | 0.17 | 1194 | 27 | 1168 | 32 | 4.92 | 1.17 | 0.0788 | 0.80 | 2.209 | 1.42 | 0.203 | 1.17 | 0.83 |
| RM30-11 | BZC | –0.03 | 142 | 122 | 0.89 | 1378 | 41 | 1383 | 90 | 4.20 | 1.52 | 0.0878 | 2.36 | 2.894 | 2.80 | 0.238 | 1.52 | 0.54 |
| RM30-12 | DUC | 0.00 | 2091 | 100 | 0.05 | 1184 | 48 | 1203 | 28 | 4.95 | 2.11 | 0.0802 | 0.71 | 2.233 | 2.23 | 0.202 | 2.11 | 0.95 |
| RM30B-1 | DUC | –0.01 | 944 | 15 | 0.02 | 1138 | 28 | 1199 | 62 | 5.16 | 1.29 | 0.0800 | 1.58 | 2.139 | 2.04 | 0.194 | 1.29 | 0.63 |
| RM30B-2 | DUC | –0.01 | 966 | 10 | 0.01 | 1163 | 27 | 1174 | 45 | 5.06 | 1.20 | 0.0790 | 1.14 | 2.157 | 1.66 | 0.198 | 1.20 | 0.73 |
| RM30B-3 | DUC | 0.00 | 1391 | 16 | 0.01 | 1199 | 27 | 1210 | 51 | 4.89 | 1.16 | 0.0805 | 1.29 | 2.271 | 1.74 | 0.205 | 1.16 | 0.67 |
| RM30B-4A | DUC | –0.01 | 695 | 114 | 0.17 | 1184 | 29 | 1273 | 58 | 4.94 | 1.24 | 0.0831 | 1.48 | 2.322 | 1.93 | 0.203 | 1.24 | 0.64 |
| RM30B-4B | BZI | –0.07 | 98 | 178 | 1.87 | 1052 | 37 | 1206 | 138 | 5.61 | 1.79 | 0.0798 | 3.53 | 1.979 | 3.93 | 0.179 | 1.79 | 0.46 |
| RM30B-5 | DUI | –0.02 | 276 | 205 | 0.77 | 1115 | 30 | 976 | 89 | 5.33 | 1.39 | 0.0714 | 2.18 | 1.855 | 2.58 | 0.188 | 1.39 | 0.54 |
| RM30B-6 | DUI | 0.13 | 897 | 109 | 0.13 | 1058 | 25 | 992 | 56 | 5.62 | 1.24 | 0.0733 | 1.26 | 1.771 | 1.85 | 0.178 | 1.24 | 0.67 |
| RM30B-7 | BZC | –0.07 | 130 | 341 | 2.72 | 1114 | 39 | 1041 | 147 | 5.32 | 1.78 | 0.0734 | 3.66 | 1.918 | 4.04 | 0.188 | 1.78 | 0.44 |
| RM30B-7B | DUR | –0.01 | 527 | 148 | 0.29 | 1027 | 25 | 996 | 65 | 5.80 | 1.26 | 0.0723 | 1.60 | 1.721 | 2.03 | 0.172 | 1.26 | 0.62 |
| RM30B-8X | BZC | –0.08 | 99 | 207 | 2.15 | 961 | 34 | 948 | 157 | 6.23 | 1.81 | 0.0700 | 3.88 | 1.566 | 4.24 | 0.161 | 1.81 | 0.43 |
| RM30B-9 | DZC | 0.10 | 438 | 142 | 0.34 | 1365 | 38 | 1919 | 137 | 4.10 | 1.30 | 0.1184 | 3.76 | 3.953 | 4.04 | 0.244 | 1.30 | 0.32 |
| RM30B-10 | DUC | –0.01 | 525 | 12 | 0.02 | 1117 | 27 | 1205 | 60 | 5.27 | 1.27 | 0.0802 | 1.52 | 2.103 | 1.97 | 0.190 | 1.27 | 0.64 |
| RM30B-11 | DEC | 0.32 | 640 | 56 | 0.09 | 1201 | 30 | 1317 | 91 | 4.84 | 1.26 | 0.0878 | 2.04 | 2.416 | 2.65 | 0.206 | 1.26 | 0.47 |
| RM30B-12 | DUC | 0.11 | 823 | 33 | 0.04 | 1065 | 27 | 1118 | 54 | 5.55 | 1.33 | 0.0778 | 1.18 | 1.908 | 1.89 | 0.180 | 1.33 | 0.70 |
| RM30B-12B | BZR | –0.07 | 105 | 201 | 1.99 | 1104 | 49 | 906 | 178 | 5.40 | 2.26 | 0.0687 | 4.37 | 1.769 | 4.89 | 0.185 | 2.26 | 0.46 |
| RM30B-13 | DUC | 0.07 | 1190 | 10 | 0.01 | 1239 | 28 | 1220 | 44 | 4.72 | 1.18 | 0.0816 | 0.99 | 2.363 | 1.63 | 0.212 | 1.19 | 0.73 |
| RM30B-14 | DUC | 0.61 | 672 | 52 | 0.08 | 1581 | 50 | 2653 | 42 | 3.27 | 1.29 | 0.1855 | 0.88 | 7.536 | 1.81 | 0.304 | 1.30 | 0.72 |
| RM30B-14B | BZR | –0.07 | 116 | 200 | 1.78 | 995 | 34 | 1108 | 140 | 5.97 | 1.76 | 0.0759 | 3.54 | 1.769 | 3.93 | 0.168 | 1.76 | 0.45 |
| RM30B-15 | DZC | 0.12 | 258 | 85 | 0.34 | 1367 | 37 | 1340 | 115 | 4.24 | 1.39 | 0.0871 | 2.85 | 2.799 | 3.29 | 0.236 | 1.39 | 0.42 |
| RM30B-8B | DUR | 0.08 | 615 | 115 | 0.19 | 1043 | 26 | 922 | 73 | 5.72 | 1.27 | 0.0704 | 1.66 | 1.682 | 2.18 | 0.175 | 1.27 | 0.58 |
| RM30B-16 | DZC | 0.06 | 606 | 3100 | 5.28 | 1562 | 37 | 1500 | 47 | 3.66 | 1.22 | 0.0941 | 1.22 | 3.525 | 1.74 | 0.273 | 1.22 | 0.70 |
| RM30C-1 | GEI | –0.01 | 1204 | 607 | 0.52 | 1132 | 10 | 1179 | 37 | 5.20 | 0.43 | 0.0792 | 0.93 | 2.103 | 1.02 | 0.192 | 0.43 | 0.42 |
| RM30C-2 | GEI | –0.01 | 867 | 303 | 0.36 | 1207 | 11 | 1199 | 42 | 4.86 | 0.48 | 0.0800 | 1.05 | 2.272 | 1.16 | 0.206 | 0.48 | 0.41 |
| RM30C-3 | DEC | –0.01 | 853 | 661 | 0.80 | 1094 | 11 | 1123 | 44 | 5.40 | 0.51 | 0.0770 | 1.11 | 1.968 | 1.22 | 0.185 | 0.51 | 0.42 |
| RM30C-4 | DUC | 0.42 | 2288 | 1399 | 0.63 | 1254 | 11 | 1530 | 93 | 4.57 | 0.37 | 0.0987 | 1.75 | 2.858 | 2.51 | 0.218 | 0.41 | 0.16 |
| RM30C-5 | GEI | –0.01 | 634 | 199 | 0.32 | 1121 | 13 | 1223 | 49 | 5.24 | 0.58 | 0.0810 | 1.26 | 2.133 | 1.38 | 0.191 | 0.58 | 0.42 |
| RM30C-6 | BUR | –0.02 | 293 | 82 | 0.29 | 1177 | 17 | 1142 | 72 | 5.00 | 0.74 | 0.0777 | 1.82 | 2.146 | 1.96 | 0.200 | 0.74 | 0.38 |
| RM30C-7 | BUR | –0.05 | 143 | 38 | 0.28 | 1074 | 26 | 1148 | 147 | 5.50 | 1.19 | 0.0776 | 3.72 | 1.957 | 3.88 | 0.182 | 1.19 | 0.31 |
| RM30C-8 | BZC | 0.14 | 173 | 111 | 0.66 | 1431 | 26 | 1582 | 80 | 3.98 | 0.90 | 0.0990 | 1.93 | 3.380 | 2.31 | 0.251 | 0.91 | 0.39 |
| RM30C-9 | DUC | 0.18 | 2752 | 185 | 0.07 | 1199 | 8 | 1479 | 28 | 4.81 | 0.28 | 0.0941 | 0.54 | 2.648 | 0.78 | 0.207 | 0.29 | 0.37 |
| RM30C-10 | GZI | –0.01 | 602 | 196 | 0.34 | 1163 | 11 | 1172 | 49 | 5.06 | 0.50 | 0.0789 | 1.23 | 2.154 | 1.33 | 0.198 | 0.50 | 0.38 |
| RM30C-11 | GZC | –0.01 | 847 | 548 | 0.67 | 1080 | 11 | 1176 | 44 | 5.46 | 0.51 | 0.0791 | 1.11 | 1.999 | 1.22 | 0.183 | 0.51 | 0.42 |
| RM30C-12 | DUC | 1.98 | 1938 | 787 | 0.42 | 1188 | 35 | 1782 | 403 | 4.69 | 0.43 | 0.1261 | 9.08 | 3.141 | 11.06 | 0.209 | 0.49 | 0.04 |
| RM30C-13 | DEI | 0.03 | 1051 | 349 | 0.34 | 1180 | 10 | 1224 | 37 | 4.97 | 0.44 | 0.0813 | 0.93 | 2.251 | 1.05 | 0.201 | 0.44 | 0.42 |
| RM30C-14 | DEC | –0.01 | 493 | 172 | 0.36 | 1129 | 15 | 1206 | 57 | 5.21 | 0.69 | 0.0803 | 1.45 | 2.128 | 1.60 | 0.192 | 0.69 | 0.43 |
| RM30C-15 | DUC | 0.00 | 2125 | 211 | 0.10 | 1211 | 9 | 1432 | 25 | 4.79 | 0.34 | 0.0903 | 0.67 | 2.602 | 0.75 | 0.209 | 0.34 | 0.46 |
| CAR-1 | GEI | –0.14 | 66 | 34 | 0.53 | 700 | 33 | 569 | 239 | 8.77 | 2.39 | 0.0579 | 5.60 | 0.929 | 5.98 | 0.114 | 2.39 | 0.40 |
| CAR-1B | BUR | –0.32 | 49 | 1 | 0.02 | 470 | 43 | 468 | 365 | 13.25 | 4.67 | 0.0538 | 8.64 | 0.589 | 9.47 | 0.076 | 4.67 | 0.49 |
| CAR-2 | GZC | 0.70 | 93 | 100 | 1.10 | 715 | 28 | 572 | 382 | 8.51 | 1.95 | 0.0648 | 5.52 | 0.951 | 9.00 | 0.117 | 2.00 | 0.22 |
| CAR-3 | GEC | 1.10 | 62 | 58 | 0.96 | 756 | 34 | 147 | 652 | 8.11 | 2.28 | 0.0577 | 6.12 | 0.824 | 14.10 | 0.122 | 2.39 | 0.17 |
| CAR-4 | DUC | 0.16 | 564 | 753 | 1.38 | 640 | 17 | 685 | 112 | 9.55 | 1.32 | 0.0636 | 2.08 | 0.898 | 2.94 | 0.105 | 1.32 | 0.45 |
| CAR-5 | GZC | –0.08 | 121 | 66 | 0.57 | 738 | 29 | 859 | 169 | 8.22 | 2.02 | 0.0670 | 4.10 | 1.136 | 4.54 | 0.122 | 2.02 | 0.45 |
| CAR-6 | GZC | –0.12 | 83 | 83 | 1.04 | 753 | 31 | 797 | 211 | 8.06 | 2.07 | 0.0647 | 5.12 | 1.125 | 5.45 | 0.124 | 2.07 | 0.38 |
| CAR-7 | DZC | –0.03 | 295 | 348 | 1.22 | 702 | 21 | 809 | 110 | 8.66 | 1.53 | 0.0658 | 2.64 | 1.052 | 3.04 | 0.115 | 1.53 | 0.50 |
| CAR-8A | DZC | –0.02 | 716 | 792 | 1.14 | 649 | 16 | 751 | 76 | 9.40 | 1.27 | 0.0642 | 1.80 | 0.943 | 2.20 | 0.106 | 1.27 | 0.58 |
| CAR-8B | BZR | –0.45 | 30 | 18 | 0.62 | 718 | 50 | 1008 | 361 | 8.43 | 3.50 | 0.0691 | 9.39 | 1.196 | 9.56 | 0.119 | 3.50 | 0.37 |
| CAR-9 | GZC | –0.16 | 64 | 45 | 0.72 | 735 | 33 | 811 | 242 | 8.27 | 2.30 | 0.0648 | 5.91 | 1.104 | 6.22 | 0.121 | 2.30 | 0.37 |
| CAR-10 | DUC | 0.13 | 681 | 918 | 1.39 | 481 | 13 | 445 | 121 | 12.91 | 1.34 | 0.0569 | 2.36 | 0.595 | 3.04 | 0.077 | 1.34 | 0.44 |
| CAR-11 | DZC | –0.05 | 210 | 200 | 0.99 | 750 | 25 | 733 | 140 | 8.11 | 1.72 | 0.0633 | 3.33 | 1.084 | 3.73 | 0.123 | 1.72 | 0.46 |
| CAR-11B | GZI | –0.22 | 48 | 30 | 0.66 | 728 | 40 | 386 | 321 | 8.48 | 2.80 | 0.0526 | 7.39 | 0.886 | 7.68 | 0.118 | 2.80 | 0.36 |

*Note:* Zone type indicates the nature of zoning at the analytical spot. Note that the abbreviations in the zone type column are concatenated. Abbreviations: B—bright in cathodoluminescence; C—core; D—dark; E—euhedral (~oscillatory) zoned; G—gray; I—interior (not a distinct core) ; R—rim; U—weakly zoned or unzoned; Z—distinctly zoned.
†$^{207}$Pb-corrected; §$^{204}$Pb-corrected; #radiogenic

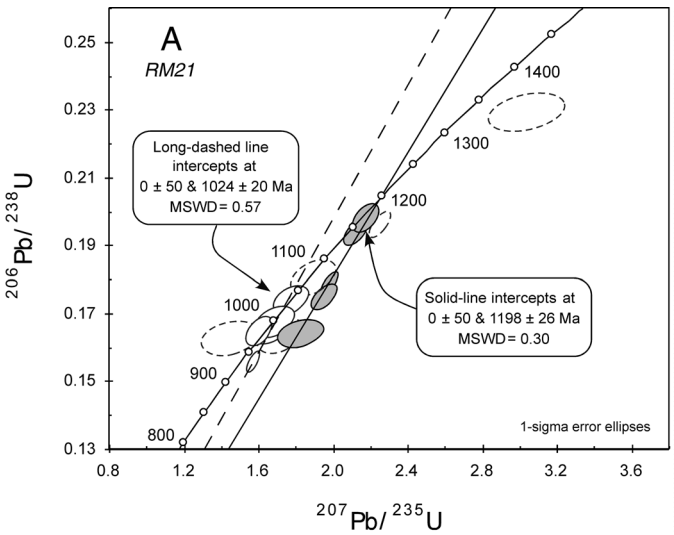
A
RM21
Long-dashed line intercepts at 0 ± 50 & 1024 ± 20 Ma MSWD= 0.57
Solid-line intercepts at 0 ± 50 & 1198 ± 26 Ma MSWD= 0.30
1-sigma error ellipses
800
900
1000
1100
1200
1300
1400
$^{206}Pb/^{238}U$
$^{207}Pb/^{235}U$

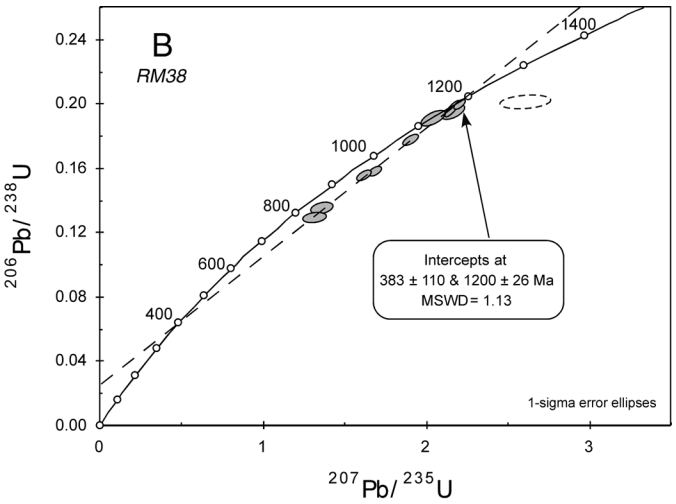
B
RM38
Intercepts at 383 ± 110 & 1200 ± 26 Ma MSWD= 1.13
1-sigma error ellipses
400
600
800
1000
1200
1400
$^{206}Pb/^{238}U$
$^{207}Pb/^{235}U$

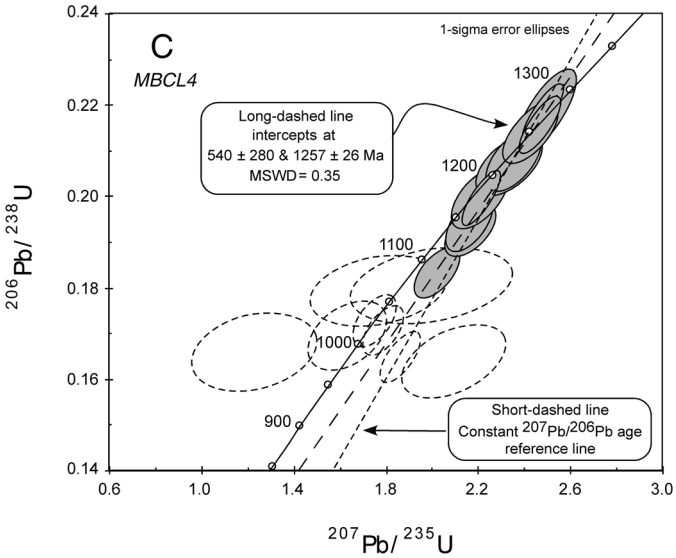
C
MBCL4
1-sigma error ellipses
Long-dashed line intercepts at 540 ± 280 & 1257 ± 26 Ma MSWD= 0.35
Short-dashed line Constant $^{207}Pb/^{206}Pb$ age reference line
900
1000
1100
1200
1300
$^{206}Pb/^{238}U$
$^{207}Pb/^{235}U$

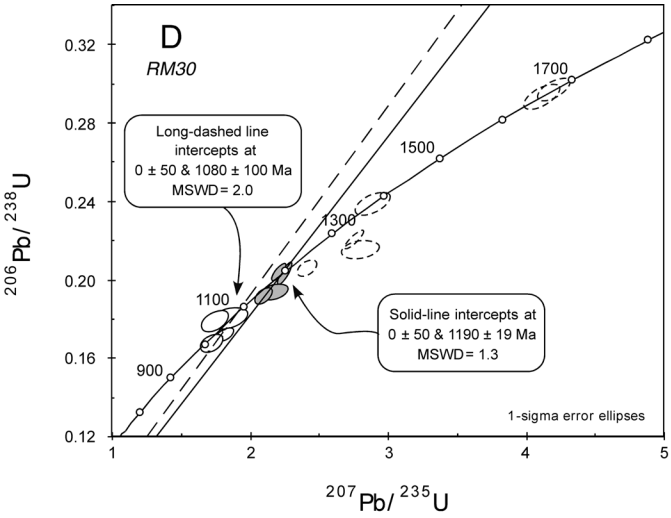
D
RM30
Long-dashed line intercepts at 0 ± 50 & 1080 ± 100 Ma MSWD= 2.0
Solid-line intercepts at 0 ± 50 & 1190 ± 19 Ma MSWD= 1.3
1-sigma error ellipses
900
1100
1300
1500
1700
$^{206}Pb/^{238}U$
$^{207}Pb/^{235}U$

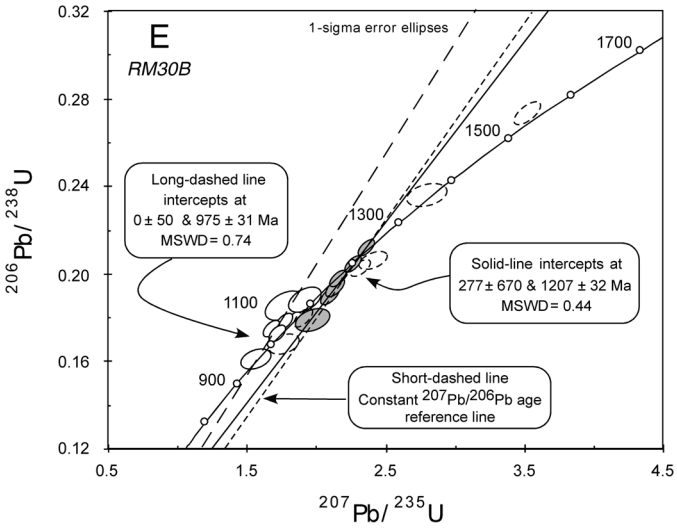
E
RM30B
1-sigma error ellipses
Long-dashed line intercepts at 0 ± 50 & 975 ± 31 Ma MSWD= 0.74
Solid-line intercepts at 277 ± 670 & 1207 ± 32 Ma MSWD= 0.44
Short-dashed line Constant $^{207}Pb/^{206}Pb$ age reference line
900
1100
1300
1500
1700
$^{206}Pb/^{238}U$
$^{207}Pb/^{235}U$

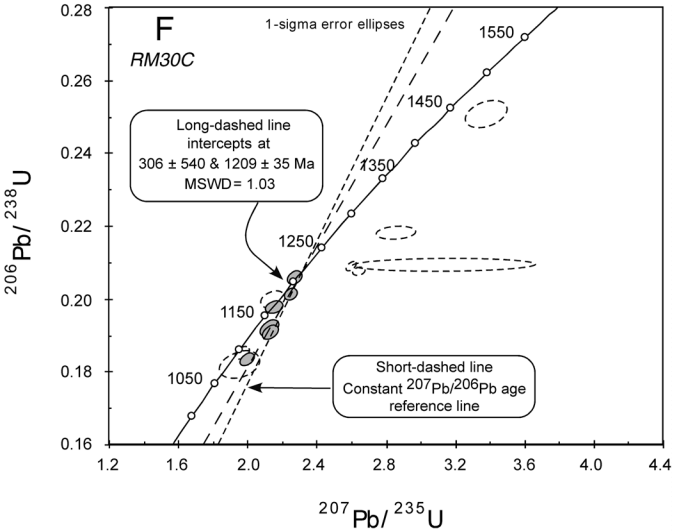
F
RM30C
1-sigma error ellipses
Long-dashed line intercepts at 306 ± 540 & 1209 ± 35 Ma MSWD= 1.03
Short-dashed line Constant $^{207}Pb/^{206}Pb$ age reference line
1050
1150
1250
1350
1450
1550
$^{206}Pb/^{238}U$
$^{207}Pb/^{235}U$

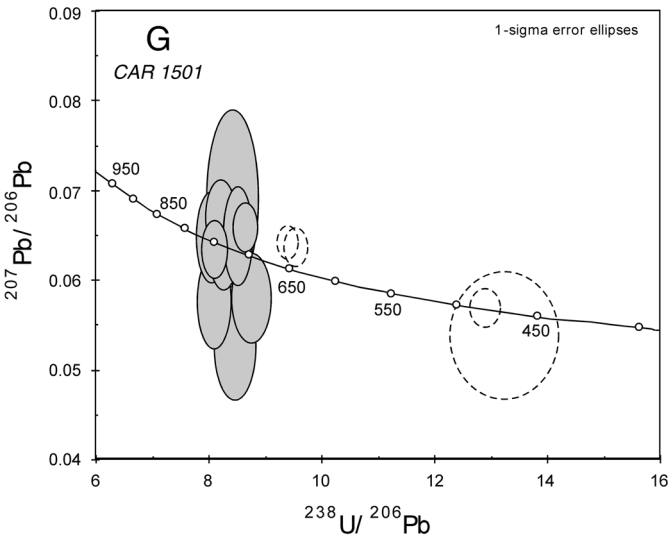


Figure 9. Concordia plots displaying U-Pb data for analyzed samples. Ellipses represent 1σ uncertainty for individual analyses. Gray ellipses were used to calculate discordia regressions that we interpret to represent ages of magmatic crystallization and Pb loss; open ellipses enclosed by solid lines are regions interpreted as metamorphic, with upper intercepts taken to be the age of metamorphism; and ellipses enclosed by dashed lines are inherited, detrital, or, in some cases, of uncertain origin (possibly a 1.1- to 1.2-Ga metamorphic event?). Errors in the calculated intercepts are 2σ Solid lines, which extend from the origin through the approximate upper intercept for magmatic points (i.e., they represent constant $^{207}Pb/^{206}Pb$ age), are for reference.? (A–F) Conventional concordia plots; (G) Tera-Wasserburg concordia plot for CAR 1501 without common Pb correction.

$^{207}Pb/^{206}Pb$ age of 1245 ± 18 Ma (MSWD, 1.2); as with RM38, the younger age and higher MSWD are consistent with the well-defined discordia with a nonzero lower intercept. Probable metamorphic zones yielded imprecise and, in some cases, strongly discordant or reversely discordant results, but an age of ca. 1.0 Ga is suggested.

## RM30 Samples (Highway 143 Road Cut

Zircons from all three RM30 samples are complexly zoned, with unzoned to weakly zoned rims and, in most cases, multiple distinct interior zones. The best-defined population in all three samples is from interior zones with ages of ca. 1.20 Ga; other interior zones have diverse older ages, suggesting that they represent inherited and/or detrital cores.

### *RM30—Felsic Orthogneiss(?)*

All zircons from RM30 have thin to thick, dark interior zones. Many have some small, concentrically zoned cores inside the dark zones, and all have thin to thick bright rims (Fig. 8, D). Four analyses, three from small euhedral-zoned cores and one from a dark, weakly zoned interior, have $^{207}Pb/^{206}Pb$ ages of 1168 to 1239 Ma and yield a pooled age of 1190 ± 19 Ma (MSWD, 1.3) (Fig. 9, D). Four analyses, three of bright rim zones and a fourth from an interior, give a mean $^{207}Pb/^{206}Pb$ age of 1080 ± 100 Ma. Six zoned cores range in $^{207}Pb/^{206}Pb$ age from 1320 to 1672 Ma, with two concordant at 1658 Ma and 1672 Ma. These cores are presumably either inherited or detrital.

### *RM30B—Banded Paragneiss(?)*

Some zircons from this sample have tiny dark cores, and many have larger concentrically zoned cores (Fig. 8, E) or dark, unzoned to weakly zoned interiors. Almost all of these interiors are surrounded by thick bright, weakly zoned regions that in some cases extend to the rims and in others are surrounded by thin to thick dark outer rims.

Seven analyses that probably represent metamorphic growth (including unzoned dark and bright interiors and rims) have a mean $^{207}Pb/^{206}Pb$ age of 975 ± 31 Ma (MSWD, 0.74) (Fig. 9, E). Six points from weakly to strongly zoned interiors and distinct cores define a discordia with intercepts of 1207 ± 32 Ma and 277 ± 670 Ma (MSWD, 0.44); these points have a mean $^{207}Pb/^{206}Pb$ age of 1211 ± 34 Ma (MSWD, 1.5). Four cores range in $^{207}Pb/^{206}Pb$ age from 1273 to 1500 Ma, another is 1919 Ma, and a sixth is 2653 Ma. If this is indeed a metasedimentary rock, as suggested previously, both the 1200-Ma points and the older ages represent detrital zircon; if the protolith is plutonic or volcanic, 1200 Ma is presumably the crystallization age, and the older ages may be inherited.

### *RM30C—Mafic, Orthopyroxene-Bearing Banded Orthogneiss*

RM30C zircons have euhedral-zoned magmatic interiors, commonly with sector zoning (Fig. 8, F). Well-defined dark or bright cores are fairly common, and most grains have bright, thin metamorphic rims. Seven points from magmatic-like, euhedral-zoned regions define a discordia with intercepts of 1209 ± 35 Ma and 306 ± 540 Ma (MSWD, 1.3) (Fig. 9, F). The same points have a have a mean $^{207}Pb/^{206}Pb$ age of 1197 ± 24 Ma (MSWD, 1.3). One analysis from a similar area falls off the concordia and yields a younger $^{207}Pb/^{206}Pb$ age of 1123 ± 44 Ma. Two imprecise analyses from rim zones that appear to document metamorphic growth have $^{207}Pb/^{206}Pb$ ages of 1142 ± 72 Ma and 1148 ± 147 Ma. These may suggest an older episode that is evident from metamorphic zones in other samples, or there may have been slight beam overlap with interiors that are older and richer in U. Four inherited (or detrital?) cores have $^{207}Pb/^{206}Pb$ ages between 1432 Ma and 1582 Ma, and another is highly discordant and has an imprecise $^{207}Pb/^{206}Pb$ age of 1782 ± 201 Ma. That these cores are invariably armored by thick magmatic overgrowths suggests that they are inherited.

The zircon data have implications for the interpretation of the RM30 exposure. As discussed previously, field relations suggest that either all three lithologies are part of a depositional sequence, or the protolith of felsic gneiss RM30 was a dike or sill that intruded the banded gneisses. Elemental chemistry is most consistent with RM30 and RM30C being felsic and mafic

meta-igneous rocks and RM30B being a metamorphosed feldspathic sandstone. The strikingly similar patterns of zircon zonation and ages are consistent with all three samples being part of a 1.2-Ga volcanic/volcaniclastic sediment sequence that incorporated detrital and xenocrystic zircons.

### CAR 1501—Meadlock Mountain Mafic, Orthopyroxene-Free Orthogneiss

Zircons from the sample CAR 1501 have euhedral-zoned interiors and thin to fairly thick bright rims (Fig. 8, G). Twelve data points from the magmatic zones are concordant (or nearly so) and fall between 640 Ma and 756 Ma (Fig. 9, G). When pooled after excluding two young outliers (640 Ma and 649 Ma, possibly reflecting Pb loss), the data yield a weighted mean $^{206}Pb/^{238}U$ age of 728 ± 16 Ma (MSWD, 2.1)—a magmatic age completely different from the remainder of the samples but essentially identical to the 734 ± 26-Ma Rb-Sr age determined by Goldberg et al. (1986) for Bakersville dikes. Two points that apparently represent metamorphic growth are concordant at ca. 475 Ma.

## CONCLUSIONS

### Age of Mars Hill Crust

Our new data further substantiate the notion that the MHT represents Paleoproterozoic crust. Although we did not date any additional samples that crystallized before 1.3 Ga, ca. 2-Ga Sm-Nd model ages for mafic and felsic samples and abundant inherited and detrital zircons with 1.6- to 1.9-Ga ages support the ancient heritage suggested by Monrad ands Gulley (1983), Sinha et al. (1996), Fullagar and Gulley (1999), and Carrigan et al. (2003). The evidence suggests that the MHT is Paleoproterozoic crust that was intensely reactivated at 1.20 Ga.

### Two Generations of Mafic Rocks

The presence in the MHT of the Neoproterozoic Bakersville dike swarm is well established (e.g., Goldberg et al., 1986); however, the age and relationships of other metabasites have been more problematic. The 1.20-Ga age of mafic sample RM30C demonstrates that at least some of the mafic rocks of the MHT are much older than the Bakersville dikes.

Our data suggest that MHT mafic rocks may be roughly divided into two groups, based on the presence or absence of opx. We interpret the presence of opx to reflect granulite-facies metamorphism, probably during the Grenville orogeny; the absence of opx indicates that the rock may have escaped this metamorphism and suggests that its protolith may be post-Grenville. Gulley (1982) and Rainey (1989) demonstrated that in some areas, Bakersville dikes contain opx interpreted to be of metamorphic origin, indicating post-Neoproterozoic granulite-facies metamorphism. Thus, presence or absence of opx is certainly not an entirely reliable discriminator of Neoproterozoic mafic rocks from older samples. However, for the limited number of samples that we have studied, it appears to distinguish populations that are otherwise distinct in petrogenesis and probably in age. The age of RM30C is 1.20 Ga, whereas that of opx-free garnet amphibolite CAR 1501 is 0.73 Ga, identical in age to the Bakersville dikes. The two analyzed opx-free samples have Sr and Nd isotope ratios that match Bakersville dikes (Goldberg et al., 1986; Goldberg and Dallmeyer, 1997); the two analyzed opx-bearing samples have very different ratios that suggest much greater age. The four opx-free samples plot on tectonic discrimination diagrams as within-plate basalts, consistent with Neoproterozoic, rift-related origin, whereas the three opx-bearing samples plot in distinct fields, generally as arc-related basalts. The opx-free samples have normal Th/U ratios, in contrast to the elevated ratios of the opx-bearing samples.

Regardless of the general applicability of the distinction between opx-bearing and opx-free mafic rocks, it is evident that metamorphosed mafic bodies in the MHT reflect both Neoproterozoic, rift-related magmatism and one or more generations of early and possibly pre-Grenville magmatism.

### Ages of Magmatism and Metamorphism

Carrigan's recent work (Carrigan, 2000; Carrigan et al., 2003) verified the existence of 1.8-Ga felsic igneous rock at Roan Mountain, as suggested by Monrad and Gulley (1983), and indicated that somewhat younger (ca. 1.6-Ga) Paleproterozoic rock and 1.2-Ga Mesoproterozoic rock were also present. Our new data suggest widespread felsic and mafic magmatism of early Grenville age. By far the dominant magmatism occurred at 1.20 ± 0.01 Ma. A single sample documents a 1.25-Ga magmatic event. The MHT apparently escaped mid- and late Grenville magmatism (post-1.18 Ga), but it was heavily intruded by mafic magma during incipient rifting at 0.73 Ga.

Although generally imprecise, our data for zones interpreted to be metamorphic are consistent with the 1.03-Ga age estimated by Carrigan et al. (2003) for peak metamorphism of basement rocks in the Blue Ridge. There is also a possible suggestion of an earlier episode of metamorphic growth at or prior to ca. 1.1 Ga. Carrigan et al. (2003) found no distinguishable differences in ages of metamorphic rims between Eastern Blue Ridge, Western Blue Ridge, and the MHT. There is also evidence for Ordovician (Taconic) metamorphism from 470-Ma zircon overgrowths from Neoproterozoic sample CAR 1501. There is no other direct evidence for Paleozoic metamorphism in our zircon data, but lower discordia intercepts of Paleozoic age and thin, undated rims on zircons from several samples that were observed under cathodoluminescence may reflect Paleozoic events.

### Geologic Evolution

The early stages of the history of the MHT are poorly defined, having been obscured by subsequent events. Available

evidence suggests formation of juvenile, probably arc-related crust during the Paleoproterozoic. The Sm-Nd model ages of samples other than Neoproterozoic mafic rocks, the magmatic crystallization age of RM1, and U-Pb ages of detrital and inherited zircons from several samples fall in the range 1.9 ± 0.2 Ga.

A major, possibly bimodal magmatic episode in early Grenville time (1.2 Ga) appears not to have added much new crust, based on Sm-Nd isotopic compositions of samples of this age. The triggering mechanism remains uncertain, as does the relationship between magmatism and sedimentation. Ages of detrital zircon suggest that sedimentation was roughly coeval with magmatism, but neither geochronology nor observed field relations permit us to say whether they were strictly simultaneous (interlayered volcanic and sedimentary strata), sediments were deposited on a slightly older igneous substrate, or sediments were intruded by slightly younger magmas. Field, elemental, and U-Pb data for the outcrop RM30 sample appears to lend credence to synchronous sedimentation and magmatism, but it is only a single exposure and far from conclusive.

Very high-grade metamorphism occurred twice, during late Grenville and Taconic episodes. The conditions attained during these episodes (Adams et al., 1995) and the widespread presence of migmatite, including in Neoproterozoic mafic rocks, suggest that local partial melting accompanied both events. We infer that complex and pervasive deformation observed in the MHT reflects both Grenville and multiple Paleozoic events. It is possible that the small-scale juxtaposition of diverse lithologies may be a consequence of deformation during anatexis. The final ductile deformation, indicated by mylonite zones, probably occurred after peak Paleozoic metamorphism.

## Constraints on Relationships to the Eastern and Western Blue Ridge

The Sm-Nd model ages, ages of magmatism, and those of detrital and inherited zircons all indicate that the MHT is a fundamentally older terrane than either the Eastern Blue Ridge or the Western Blue Ridge. It also is clearly different lithologically from the other basement rocks of the southern Blue Ridge; unlike either the Eastern Blue Ridge or Western Blue Ridge, the MHT contains metasedimentary and abundant mafic rocks. It is thus apparent that the MHT is a continental fragment, with an origin distinct from its surroundings. It is plausible that it simply represents an exposed portion of an older lower crust that underlay the more juvenile rocks of the Western Blue Ridge and possibly the Eastern Blue Ridge basement during Grenville time. Fullagar (2002) recognized contributions of older—in part, Paleoproterozoic—crust to the Blue Ridge and adjacent Inner Piedmont. Such contributions may have come from a MHT-like lower crust.

The post-1.1-Ga history of the MHT suggests linkages to the Eastern Blue Ridge and Western Blue Ridge, but the implications of these linkages remain puzzling (cf. Johnson, 1994; Raymond and Johnson, 1994; Adams and Trupe, 1997). All three areas appear to have experienced a profound metamorphic event shortly before 1.0 Ga. Both the Western Blue Ridge and the MHT—but not the Eastern Blue Ridge basement—were intruded by Neoproterozoic mafic dikes, although the MHT seems not to include any of the Neoproterozoic granites that are common in the Western Blue Ridge. Both the MHT and the Eastern Blue Ridge—but not the Western Blue Ridge—underwent similar high-grade Ordovician metamorphism. The data are consistent with, but do not require, the interpretation that all three were in fairly close proximity by late Grenville time. Because of the extent of the global Grenville orogen and of late Grenville metamorphism, the similarity in age of metamorphism may be of limited use as a geographic constraint. The distribution of Bakersville dikes appears to suggest MHT–Western Blue Ridge (but not Eastern Blue Ridge?) proximity during the Neoproterozoic, and high-grade Taconian metamorphism seems to link the Eastern Blue Ridge and MHT, but perhaps not the Western Blue Ridge, during the Ordovician.

## Constraints on Relations to Other Ancient Continental Crust

We are unaware of any other exposures of crust of similar antiquity to the MHT in the southeastern United States. The only possible Appalachian correlatives of the MHT that we are aware of are in Virginia and Maryland. The Pedlar and Lovingston massifs in the Virginia Blue Ridge both are highly diverse in terms of lithology (mafic, felsic, and some metasedimentary rocks, wide range of $SiO_2$) (e.g., Bartholomew and Lewis, 1984; Hughes et al., 1997, 2001). An upper U-Pb concordia intercept of 1.87 Ga for detrital zircon and whole-rock Pb isotope data suggesting a possible Archean source component indicate that the Stage Road layered gneiss, a unit of the Lovingston massif, records input from material that was much older than Grenville (Pettingill et al., 1984; Sinha and Bartholomew, 1984; Sinha et al., 1996). However, the reported Sm-Nd isotopic compositions of analyzed samples of the Stage Road gneiss and other Pedlar and Lovingston lithologies ($\varepsilon_{Nd} > 0$ at 1.1 Ga) (Pettingill et al., 1984) is nowhere near as evolved as that which we have found so far in the MHT. The Goochland terrane, which lies to the east in the Piedmont zone and is of uncertain origin, also is lithologically diverse, but there is no evidence that it includes protoliths much older than Grenville age (no pre-Grenville zircon ages; $\varepsilon_{Nd,\ 1.1\ Ga} \sim 0$, $T_{DM} \sim 1.4$ Ga) (Owens and Samson, 2001). Aleinikoff et al. (this volume) report 1.25-Ga ages for felsic gneisses of the Baltimore Gneiss in the Maryland Piedmont, similar to the dominant MHT magmatic age population. Like the MHT, the Baltimore Gneiss includes both mafic and felsic rocks. However, there appears to be no zircon evidence for Paleoproterozoic precursor crust (no old inheritance), and Pb isotope data reported by Sinha et al. (1996) for Baltimore Gneiss are consistent with other central and southern Appalachian basement but not with the MHT. There are no reported Nd isotopic data for the Baltimore Gneiss.

The nearest known crust of Paleoproterozoic origin is in the Penokean Province near the western Great Lakes. Paleoproterozoic crust is also exposed in the southwestern United States, including parts of the Mojave, Yavapai, and Mazatzal terranes (e.g., Karlstrom et al., 1999). These areas contain diverse lithologies and have compatible estimated crustal formation ages ($T_{DM}$ values of ca. 2 Ga). The MHT is separated from all of these Paleoproterozoic exposures by a vast tract of early Mesoproterozoic rocks (ca. 1.4- to 1.5-Ga magmatic crystallization ages) that is interpreted to represent juvenile crust ($T_{DM}$ values are only very slightly older) (Van Schmus et al., 1996). If the MHT was once a part of a Paleoproterozoic Laurentian crustal block with the Great Lakes and/or southwestern terranes, and if the midcontinent province is juvenile, then the MHT may be a rifted Laurentian fragment and the midcontinent province an enormous expanse of rift-fill crust. The Pb isotope ratios of southern Appalachian basement have been used as evidence that southern Appalachian crust in general did not originate in its current position with respect to Laurentia, and existing data for the MHT suggest that it is even more distinct from nearby parts of the continent than is true for the rest of the southern Appalachians (Sinha et al., 1996; Sinha and McLelland, 1999; Loewy et al., 2002). An origin adjacent to a distant part of Laurentia might explain this and other discrepancies. Alternatively, the MHT may be an orphan fragment of crust removed from a larger Paleoproterozoic terrane now exposed on another continent, perhaps in West Africa or South America (Rogers, 1996; Tosdal, 1996; Ruiz et al., 1999; Loewy et al., 2002; Pisarevsky et al., 2003).

## ACKNOWLEDGMENTS

Kevin Stewart, Carl Merschat, Mark Carter, Mark Adams, and Loren Raymond kindly contributed valuable insights and time in the field with us; we benefited enormously from the work they had done in this region and their generosity in sharing it with us. Brendan Bream, Bob Hatcher, and Jerry Bartholomew all contributed ideas about Appalachian tectonics that contributed to our perspective on Mars Hill problems, and Bream also donated his time and skills in the SHRIMP lab. Richard Tollo, Kevin Stewart, Paul Mueller, John Aleinikoff, and Jerry Bartholomew provided careful reviews of this text that helped us to strengthen and clarify it; the interpretations remain our own, however, and the reviewers should share no blame. The work was supported by NSF grant EAR98-14801 and a Eugene H. Vaughan Jr., research scholarship awarded to SEO by the Vanderbilt Department of Geology.

## REFERENCES CITED

Adams, M.G., and Trupe, C.H., 1997, Conditions and timing of metamorphism in the Blue Ridge thrust complex, northwestern North Carolina and western Tennessee, *in* Stewart, K.G., et al., eds., Paleozoic structure, metamorphism, and tectonics of the Blue Ridge of western North Carolina: Carolina Geological Society Field Trip and Annual Meeting, p. 33–47.

Adams, M.G., Stewart, K.G., Trupe, C.H., and Willard, R.A., 1995, Tectonic significance of high-pressure metamorphic rocks and dextral strike-slip faulting along the Taconic suture, *in* Hibbard, J.P., et al., eds., Current perspectives in the Appalachian-Caledonian orogen: Geological Association of Canada, Special Paper 41, p. 21–42.

Bacon, C.R., Persing, H.M., Wooden, J.L., and Ireland, T.R., 2000, Late Pleistocene granodiorite beneath Crater Lake caldera, Oregon, dated by ion microprobe: Geology, v. 28, p. 467–470.

Bartholomew, M.J., and Lewis, S.E., 1984, Evolution of Grenville massifs in the Blue Ridge geologic province, southern and central Appalachians, *in* Bartholomew, M.J., ed., The Grenville Event in the Appalachians and related topics: Boulder, Colorado, Geological Society of America Special Paper 194, p. 229–254.

Bartholomew, M.J., and Lewis, S.E., 1988, Peregrination of middle Proterozoic massifs and terranes within the Appalachian orogen, eastern USA: Trabajos de Geología, v. 17, p. 155–165.

Bartholomew, M.J., and Lewis, S.E., 1992, Appalachian Grenville massifs: Pre-Appalachian translational tectonics, *in* Mason, R., ed., Basement tectonics 7: Dordrecht, The Netherlands, Kluwer Academic Publishers, p. 363–374.

Boynton, W.W., 1984, Cosmochemistry of the rare earth elements, *in* Henderson, P., ed., Rare earth element geochemistry: New York, Elsevier, p. 63–114.

Brewer, R.C., and Woodward, N.B., 1988, The amphibolitic basement complex in the Blue Ridge Province of western North Carolina, Proto-Iapetus?: American Journal of Science, v. 288, p. 953–967.

Brown, P.M., Burt, E.R., II, Carpenter, P.A., Enos, R.M., Flynt, B.J., Jr., Gallagher, P.E., Horrman, C.W., Merschat, C.E., Wilson, W.F., and Parker, J.M., III, 1985, Geologic map of North Carolina: North Carolina Geological Survey, scale 1:500,000.

Carrigan, C.W., 2000, Ion microprobe geochronology of Grenville and older basement in the southern Appalachians [unpublished Master's thesis]: Nashville, TN., Vanderbilt University.

Carrigan, C.W., Miller, C.F., Hatcher, R.D., Jr., Fullagar, P.D., and Coath, C.D., 2000, Grenville basement of the southern Appalachians, NC-GA—Geochemistry and zircon ion probe geochronology: Geological Society of America Abstracts with Programs, v. 32, no. 2, p. A9.

Carrigan, C.W., Miller, C.F., Fullagar, P.D., Hatcher, R.D., Jr, Bream, B.R., and Coath, C.D., 2001, Age and geochemistry of Southern Appalachian basement, NC-SC-GA, with implications for Proterozoic and Paleozoic reconstructions: Geological Society of America Abstracts with Programs, v. 33, no. 6, p. A29.

Carrigan, C.W., Miller, C.F., Fullagar, P.D., Hatcher, R.D., Jr., Bream, B.R., and Coath, C.D., 2003, Age and geochemistry of Southern Appalachian basement, NC-SC-GA, with implications for Proterozoic and Paleozoic reconstructions: Precambrian Research, v. 120, p. 1–36.

Davis, T.L., 1993, Lithostratigraphy, structure, and metamorphism of a crystalline thrust terrane, western Inner Piedmont, North Carolina [Ph.D. thesis]: Knoxville, University of Tennessee, 245 p.

DePaolo, D.J., 1981, Neodymium isotopes in the Colorado Front Range and crust-mantle evolution in the Proterozoic: Nature, v. 291, p.193–196.

Fullagar, P.D., 2002, Evidence for early Mesoproterozoic (and older?) crust in the southern and central Appalachians of North America, *in* Rogers, J.J.W., and Santosh, M., eds., Special issue of Gondwana research on "Mesoproterozoic Supercontinent": Gondwana Research, v. 5, p. 197–203.

Fullagar, P.D., and Butler, J.R., 1979, 325–265 m.y.-old granitic plutons in the Piedmont of the southeastern Appalachians: American Journal of Science, v. 279, p. 161–185.

Fullagar, P.D., and Gulley, G.L., Jr., 1999, Pre-Grenville Uranium-Lead zircon age for the Carvers Gap Gneiss in the Western Blue Ridge of North Carolina–Tennessee: Geological Society of America Abstracts with Programs, v. 31, no. 3, p. 16.

Fullagar, P.D., Hatcher, R.D., Jr., and Merschat, C.E., 1979, 1200 m.y. old gneisses in the Blue Ridge province of North Carolina and South Carolina: Southeastern Geology, v. 20, p. 69–77.

Fullagar, P.D., Goldberg, S.A., and Butler, J.R., 1997, Nd and Sr isotopic char-

acterization of crystalline rocks from the southern Appalachian Piedmont and Blue Ridge, North Carolina and South Carolina: *in* Sinha, A.K., et al., eds., The nature of magmatism in the Appalachian orogen: Boulder, Colorado, Geological Society of America Memoir 191, p. 161–185.

Goldberg, S.A., and Dallmeyer, R.D., 1997, Chronology of Paleozoic metamorphism and deformation in the Blue Ridge thrust complex, North Carolina and Tennessee: American Journal of Science, v. 297, p. 488–526.

Goldberg, S.A., Butler, J.R., and Fullagar, P.D., 1986, The Bakersville dike swarm; geochronology and petrogenesis of late Proterozoic basaltic magmatism in the southern Appalachian Blue Ridge: American Journal of Science, v. 286, no. 5, p. 403–430.

Goldberg, S.A., Butler, J.R., Mies, J.W., and Trupe, C.H., 1989, The southern Appalachian orogen in northwestern North Carolina and adjacent states: Washington, D.C., American Geophysical Union IGC Field Trip T365, 55 p.

Gulley, G.L., Jr., 1982, The petrology of granulite facies metamorphic rocks on Roan mountain, Western Blue Ridge, NC-TN [M.S. thesis]: Chapel Hill, University of North Carolina, 163 p.

Gulley, G.L., Jr., 1985, A Proterozoic granulite-facies terrane on Roan Mountain, western Blue Ridge Belt, North Carolina-Tennessee: Geological Society of America Bulletin, v. 96, p. 1428–1439.

Hanchar, J.M., and Miller, C.F., 1993, Zircon zonation patterns and interpretation of crustal histories: Chemical Geology, v. 110, p. 1–13.

Hatcher, R.D.. Jr., 1978, Tectonics of the Western Blue Ridge, southern Appalachians: Review and speculation: America Journal of Science, v. 278, p. 276–304.

Hatcher, R.D., Jr., 1989, Tectonic synthesis of the U.S. Appalachians, *in* Hatcher, R.D., Jr., et al., eds., The geology of North America: The Appalachian-Ouachita orogen in the United States: Boulder, Colorado, Geological Society of America, v. F2, p. 511–535.

Hughes, S.S., Lewis, S.E., Bartholomew, M.J., Sinha, A.K., Hudson, T.A., and Herz, N., 1997, Chemical diversity and origin of Precambrian charnockitic rocks of the central Pedlar Massif, Grenvillian Blue Ridge Terrane, Virginia: Precambrian Research, v. 84, p. 37–46.

Hughes, S.S., Bartholomew, M.J., Lewis, S.E., Sinha, A.K., and Herz, N., 2001, Geochemistry of Precambrian charnockitic rocks of the central Lovingston Massif, Grenvillian Blue Ridge Terrane, Virginia: Geological Society of America, Abstracts with Programs, v. 33(6), p. 28.

Johnson, P.A., 1994, The Mars Hill terrane: an enigmatic southern Appalachian terrane [Senior Honors thesis]: Boone, North Carolina, Appalachian State University.

Karlstrom, K.E., Harlan, S.S., Williams, M.L., McLelland, J., Geissman, J.W., and Åhall, K.-I., 1999, Refining Rodinia: Geologic evidence for the Australia–western U.S. connection in the Proterozoic: GSA Today, v. 10, no. 9, p. 1–7.

Loewy, S.L., Connelly, J.N., and Dalziel, I.W.D., 2002, Pb isotopes as a correlation tool to constrain Rodinia reconstruction: Geological Society of America Abstracts with Programs, v. 34, no. 6, abstract 245-2, p. 558.

Ludwig, K.R., 2001, SQUID 1.02; a users manual: Berkeley, California, Berkeley Geochronology Center Special Publication no. 2.

Merschat, C.E., 1977, Geologic map and mineral resources summary of the Mars Hill quadrangle, North Carolina: North Carolina Geological Survey, Division of Land Resources, scale 1:24,000.

Merschat, C.E., and Wiener, L.S., 1990, Geology of Grenville-age basement and younger cover rocks in the west-central Blue Ridge, North Carolina: Carolina Geological Society Guidebook, 42 p.

Miller, C.F., Hanchar, J.M., Bennett, V.C., Harrison, T.M., Wark, D.A., and Foster, D.A., 1992, Source region of a batholith: Evidence from lower crustal xenoliths and inherited accessory minerals: Transactions of the Royal Society of Edinburgh: Earth Sciences (Hutton Symposium volume), v. 53, p. 49–62.

Miller, C.F., Hatcher, R.D., Jr., Harrison, T.M., Coath, C., and Gorisch, E.B., 1998, Cryptic crustal events elucidated through zone imaging and ion microprobe studies of zircon, southern Appalachian Blue Ridge, North Carolina–Georgia: Geology, v. 26, p. 419–422.

Misra, K.C., and McSween, H.Y., 1984, Mafic rocks of the southern Appalachians—A review: American Journal of Science, v. 284, p. 294–318.

Monrad, J.R., and Gulley, G.L., Jr., 1983, Age and *P-T* conditions during metamorphism of granulite-facies gneisses, Roan Mountain, NC-TN, *in* Lewis, S.E., ed., Geological Investigations in the Blue Ridge of northwestern North Carolina: Carolina Geological Society Field Trip Guidebook, article 4, p. 1–18.

Owens, B.E., and Samson, S.D., 2001, Nd-isotopic constraints on the magmatic history of the Goochland Terrane, easternmost Grenville crust in the Southern Appalachians: Geological Society of America, Abstracts with Programs, v. 33(6), p. 28.

Ownby, S.E., 2002, Ancient crust of the Mars Hill terrane, North Carolina–Tennessee: Constraints on origin from initial geochemical and geochronological studies [Senior Honors thesis]: Nashville, Tennessee, Vanderbilt University, 107 p.

Pearce, J.A., and Cann, J.R., 1973, Tectonic setting of basic volcanic rocks determined by discriminant analysis using Ti, Zr, and Y: Earth and Planetary Sciences Letters, v. 12, p. 339–349.

Pearce, J.A., Harris, N.B.W., and Tindle, A.G., 1984, Trace element discrimination diagrams for the tectonic interpretation of granitic rocks: Journal of Petrology, v. 25, p. 956–983.

Pettingill, H.S., Sinha, A.K., and Tatsumoto, M., 1984, Age and origin of anorthosites, charnockites, and granulites in the central Virginia Blue Ridge; Nd and Sr isotopic evidence: Contributions to Mineralogy and Petrology, v. 85, p. 279–291.

Pisarevsky, S.A., Wingate, M.T.D., Powell, C.M., Johnson, S., and Evans, D.A.D., 2003, Models of Rodinia assembly and fragmentation, *in* Yoshida, M., and Windley, B.F., eds., Proterozoic east Gondwana: Supercontinent assembly and breakup: Geological Society, London, Special Publication 206, p. 35–55.

Rainey, L., 1989, A study of the late Proterozoic Bakersville Suite; implications for Paleozoic metamorphism in portions of the Blue Ridge thrust complex, western North Carolina and eastern Tennessee [M.S. thesis]: Chapel Hill, University of North Carolina, 161 p.

Rankin, D.W., 1975, The continental margin of eastern North America in the southern Appalachians: The opening and closing of the proto-Atlantic Ocean: American Journal of Science, v. 275A, p. 298–336.

Raymond, L.A., 1987, Terrane amalgamation in the Blue Ridge Belt, southern Appalachian orogen, U.S.A.: Geological Society of America (Southeastern Section) Abstracts with Programs, v. 19, no. 2, p. 125.

Raymond, L.A., and Johnson, P.A., 1994, The Mars Hill terrane; an enigmatic Southern Appalachian terrane: Geological Society of America Abstracts with Programs, v. 26, no. 4, p. 59.

Raymond, L.A., Yurkovich, S.P., and McKinney, M., 1989, Block-in-matrix structures in the North Carolina Blue Ridge Belt and their significance for the tectonic history of the Southern Appalachian orogen, *in* Horton, J.W., Jr., and Rast, N. eds., Melanges and olistostromes of the U.S. Appalachians: Boulder, Colorado, Geological Society of America Special Paper 228, p. 195–215.

Rogers, J.J.W., 1996, A history of continents in the past three billion years: Journal of Geology, v. 104, p. 91–107.

Ruiz, J., Tosdal, R.M., Restrepo, P.A., and Murillo-Muneton, G., 1999, Pb isotope evidence for Colombia–southern Mexico connections in the Proterozoic, *in* Ramos, V.A., and Keppie, J.D., eds., Laurentia-Gondwana connections before Pangea: Boulder, Colorado, Geological Society of America Special Paper 336, p. 183–197.

Sinha, A.K., and Bartholomew, M.J., 1984, Evolution of the Grenville terrane in the central Virginia Appalachians, *in* Bartholomew, M.J., ed., The Grenville Event in the Appalachians and related topics: Boulder, Colorado, Geological Society of America Special Paper 194, p. 175–186.

Sinha, A.K., and McLelland, J.M., 1999, Lead isotope mapping of crustal reservoirs within the Grenville superterrane: II. Adirondack massif, New York, *in* Sinha, A.K., ed., Basement tectonics 13: Dordrecht, The Netherlands, Kluwer Academic Publishers, p. 297–312.

Sinha, A.K., Hogan, J.P., and Parks, J., 1996, Lead isotope mapping of crustal

reservoirs within the Grenville Superterrane: I. Central and southern Appalachians: American Geophysical Union Geophysical Monograph 95, p. 293–305.

Stewart, K.G., Adams, M.G., and Trupe, C.H., 1997, Paleozoic structural evolution of the Blue Ridge thrust complex, western North Carolina, *in* Stewart, K.G., et al., eds., Paleozoic structure, metamorphism, and tectonics of the Blue Ridge of western North Carolina: Carolina Geological Society Field Trip and Annual Meeting, p. 21–31.

Sun, S.S., and McDonough, W.F., 1989. Chemical and isotopic systematics of oceanic basalts: Implications for mantle compositions and processes, *in* Saunders, A.D., and Norry, M.J., eds., Magmatism in ocean basins: Geological Society of London Special Publication 42, p. 313–345.

Tosdal, R.M., 1996, The Amazon-Laurentian connection as viewed from the Middle Proterozoic rocks in the central Andes, western Bolivia and northern Chile: Tectonics, v. 15, p. 827–842.

Trupe, C.H., Adams, M.G., and Stewart, K.G., 2001, Diversity of basement rocks along the Eastern-Western Blue Ridge contact in northwestern North Carolina: Geological Society of America Abstracts with Progams, v. 33, no. 6, p. A29.

Van Schmus, W.R., Bickford, M.E., and Turek, A., 1996, Proterozoic geology of the east-central Midcontinent basement, *in* van der Pluijm, B.A., and Catacosinos, P.A., eds., Basement and basins of eastern North America: Boulder, Colorado, Geological Society of America Special Paper 308, p. 7–32.

Werner, C.D., 1987, Saxonian granulites—igneous or lithogeneous? A contribution to the geochemical diagnosis of the original rocks in high-metamorphic complexes, *in* Gerstenberger, H., ed., Contributions to the geology of the Saxonian granulite massif: Sächsisches Granulitegebirge, Zfl-Mitteilungen Nr., v. 133, p. 221–250.

Wood, D.A., 1980, The application of a Th-Ta-Hf diagram to problems of tectonomagmatic classification and to establishing the nature of crustal contamination of basaltic lavas of the British Tertiary volcanic province: Earth and Planetary Sciences Letters, v. 50, p. 11–30.

Zartman, R.E., and Doe, B.R., 1981, Plumbotectonics: The model: Tectonophysics, v. 75, p. 135–162.

Manuscript Accepted by the Society August 25, 2003

Printed in the USA